Construction and Building Materials 383 (2023) 131397

Contents lists available at ScienceDirect

Construction and Building Materials

journal homepage: www.elsevier.com/locate/conbuildmat

Effect of cross section aspect ratio and bearing surfaces treatment on the compressive strength of solid fired clay brick specimens

Albert Cabané, Luca Pelà *, Pere Roca

Department of Civil and Environmental Engineering, Universitat Politècnica de Catalunya (UPC-BarcelonaTech), Jordi Girona 1-3, 08034 Barcelona, Spain

ARTICLE INFO

Keywords:
Solid fired clay bricks
Masonry
Compressive strength
Handmade bricks
Bearing surface
Loading surface
Capping
Grinding
PTFE
Superficial treatment
Confinement

ABSTRACT

This study addresses the evaluation of the confinement effect in the experimental determination of compressive strength in solid fired clay units. The experimental campaign has focused on two different types of solid fired clay bricks, namely mechanically extruded and handmade, with a total amount of 458 specimens. The research considers different standard specimens, such as whole or half brick, and 100 × 100 × 40 mm^3 specimen, and nonstandard 40 × 40 × 40 mm^3 specimen, subjected to different standard bearing surface treatments, i.e. grinding, capping with cement mortar or gypsum plaster, placing with birch plywood or fibreboard. Additionally, two novel bearing surface treatments are proposed, i.e. covering with gypsum powder, and placing two oiled PTFE leaves. The experimental campaign has focused on four main aspects. First, the evaluation of the compressive strength value in specimens with hardening response. Second, the influence of the cross section's aspect ratio, defined as the ratio between the specimen's length and width. Third, the influence of the bearing surface treatment on the determination of the compressive strength. Fourth, the evaluation of the standard compressive strength through the comparison amongst reference standards. The results highlight and quantify the different factors that influence the confinement, while detecting differences depending on the manufacturing process of the unit. In addition, the results reveal the use of oiled PTFE leaves as a promising and fast possibility of low boundary friction to obtain the strength regardless of the specimen shape.

1. Introduction

The load-bearing capacity of masonry structures depends on their components' strength, being the compressive strength of the units one of the main important parameters [1,2]. Regardless of the type and material of the unit tested, the experimental compressive strength depends on the specimen's dimensions and the confinement produced by the friction of the press steel platens on the specimen's bearing surfaces during the test [3]. The specimen's dimensions and the confinement effect can have a remarkable influence on the experimental evaluation of the compressive strength. The experimental assessment of the compressive strength on solid fired clay units has always been a subject of debate, and many standards describe different specimen shapes, sizes and bearing surfaces treatments, showing an existing lack of consensus about a common procedure. In addition, available international standards and studies usually propose characterisation procedures and methodologies regardless the unit shape, form, material and manufacturing process.

Acquiring a full knowledge on the compressive strength of solid units is necessary to design adequate masonry structures as well as to evaluate existing ones. The experimental compressive strength characterisation of solid bricks is greatly affected by the stress developed on the specimen's bearing surface during the loading test, the reduced specimen slenderness due to its small height conditioned by the brick thickness, which can vary between 40 mm and 60 mm [4], and the cross section's aspect ratio between the length and width [5].

The analysis of the effect of the cross section's aspect ratio was addressed in few research studies available in the scientific literature. Page [6,7] studied three calcium silicate brick specimen types with the same length and height but different width, by testing them between 5 mm plywood sheets or between flexible brush platens. Khalaf et al. [5] studied four solid concrete unit specimen types by fixing the width and height and varying the length. Fódi [8] investigated three specimens of mechanically extruded solid fired clay bricks by changing their length by cutting off a part. A similar approach was followed by Salvatoni and Ugolini [9] for modern handmade solid fired clay bricks.

The stress developed on the specimen bearing surface was reported by Murray [10] in 1942, describing three possible stress conditions at

* Corresponding author.
E-mail addresses: albert.cabane@upc.edu (A. Cabané), luca.pela@upc.edu (L. Pelà), pere.roca.fabregat@upc.edu (P. Roca).

https://doi.org/10.1016/j.conbuildmat.2023.131397
Received 6 March 2023; Received in revised form 9 April 2023; Accepted 10 April 2023
Available online 17 April 2023

the bearing surfaces of the specimens: the uniform uniaxial compressive stress, the vertical compressive stress and radial tensile stress when capping materials are used due to their deformation under load, and the vertical compressive stress with restraining radial stresses induced by friction between the bearing surface and the loading press platen.

Some authors investigated how to determine a uniform uniaxial ideal "unconfined" compressive strength by testing specimens with different capping or bearing surface treatments. The steel brush bearing platens proposed by Hilsdorf [11] for concrete specimens consisted of individual filaments with a cross section of 5×3 mm^2 spaced 0.2 mm and variable length from 90 to 140 mm depending on the concrete strength, soldered together in a solid platen with 35 mm of thickness. The brushes were originally used by Kupfer et al. [12] in 1969, and reported its use by Van Mier [3], Thomas et al. [13] and Binda et al. [14,15], among others. Page [6,16] reported the use of the brush platens in calcium silicate units but with different filament section and distribution, using filaments with circular cross section of Ø5.5 mm, 120 mm long, and spaced 0.8 mm. Hussein et al. [17] modified the brush platens to test high strength concrete and proposed the use of filaments with a cross section of 5×5 mm^2 and 75 mm long, soldered in a 40 mm thickness solid platen. Schickert [18], in 1973, used the Hilsdorf brushes with a filaments cross section of 4×4 mm^2 and 90 mm long, and also proposed a piston system that divides the pressure platen into individual pistons with a cross section of 25×25 mm^2 connected to each other by elastomeric piece [19,20].

The scientific literature includes only a limited number of references about solid fired clay units, while more experimental studies can be found for concrete specimens. The first research was carried out by Gonnerman in 1924 [21], comparing the standard concrete specimens capped with cement mortar with strength ranging from 7 to 38 MPa, with alternative capping materials as gypsum or mixtures of cement and gypsum. Gonnerman [21] found that the concrete specimens had similar strength regardless of the capping material used. Purrinton et al. in 1926 [22] and McGuire in 1930 [23] proposed the use of fine sand placed in a confining container testing 14 MPa, 21 MPa, and 24 MPa concrete specimens. Purrinton et al. [22] reported that the strength of the concrete cylinders tested with sand cushion were similar to those capped with cement mortar, while McGuire [23] reported that the strength depends on the diameter of the restraining rings used to confine the sand. In 1928, Freeman [24,25] reported the use of sulphur mortar capping on 55 MPa strength concrete specimens. The research carried out in concrete specimens until the 70's focused on the comparison and validation of the specimens with strength up to 50 MPa capped with material such as cement mortar, sulphur mortar, plaster of Paris, high, medium and low strength gypsum, and mixtures of cement and gypsum (i.e. Troxel in 1941 [26], Vidal in 1942 [27], Masters et al. in 1952 [28], Werner in 1958 [29] and Saucier in 1972 [30]). Troxell [26] reported that concrete cylinders capped with high-strength gypsum or sulphur mortar had higher strength than those capped with plaster of Paris. Vidal [27] confirmed the Troxell results. Masters et al. [28] investigate the effects of the sulphur cap age and thickness on the strength, and found that higher experimental strengths were obtained in specimens with reduced thickness sulphur mortar caps. Werner [29] investigated aluminous cement mortar, plaster of Paris, mixtures of cement and plaster of Paris, high-strength gypsum, and sulphur, concluding that the use of different capping materials has greater effects on specimens made of high-strength concrete than on specimens of low-strength concrete. Saucier [30] used steel rings to confine the capping material because low-strength gypsum capping material provided lower experimental strength. In the 70's and 80's, sever studies investigated the use of an unbounded capping system composed of polychloroprene (commonly known as Neoprene ®) pads restrained by metal rings for testing of concrete specimens. Ozyildirim in 1985 [31], Carrasquillo et al. in 1987 [32] and Richardson in 1990 [33] compared the strength of the concrete specimens capped with sulphur mortar with unbonded specimens using Neoprene pads. Ozyildirim [31] and Richardson [33] tested concrete specimens up to 40 MPa and concluded that the strengths derived from the two capping methods showed no differences. Carrasquillo et al. tested specimens up to 114 MPa [32] concluding that the proposed Neoprene pad-cap system provided similar strength to those with sulphur caps. In the 90's the use of ground surfaces was incorporated to test high-strength concrete specimens and compared with the use of Neoprene pads and sulphur caps (i.e. Chojnaki et al. in 1991 [34], Pistelli et al. [35], Lessard et al. [36], and French et al. in 1993 [37], and Carino et al. in 1994 [38]). Chojnaki et al. [34] reported that for 70 MPa and 90 MPa concrete specimens there are no significant differences between specimens capped with sulphur mortar and grinded ones. Pistelli et al. [35] reported that for concrete specimens between 20 MPa and 120 MPa the use of pad-cap Neoprene system provided slightly lower strengths than grinded ones. Lessard et al. [36] reported that, for concrete specimens between 115 MPa and 130 MPa, the strength of the specimens capped with sulphur are 85% of that of the grinded ones. French et al. [37] tested concrete cylinders with grinded surfaces, capped with sulphur mortar and unbounded Neoprene cap-pads, evidencing similar strengths. French et al. [37] reported violent failure due to the energy stored in the Neoprene pads affecting the post-ultimate behaviour of the specimens. RILEM TC 148-SSC [39] presented a research carried out by 10 universities in 1997 on 45 MPa and 75 MPa concrete specimens with high and low friction loading systems. The chosen low friction loading system was based on Polytetrafluoroethylene leaves (commonly known as PTFE or Teflon ®).

The research on the bearing surface treatment influencing masonry units were initially developed by Kelch et al. in 1958 [40], Dodd et al. in 1960 [41] and Morsy in 1968 [42]. Kelch et al. [40] studied the influence of the thickness of sulphur mortar and gypsum caps on clay masonry units, reporting similar small differences. Dodd et al. [41] studied different capped materials such as cardboard, plasterboard, insulating wallboard, cement mortar and dental gypsum plaster, reporting small strength difference too. Morsy [42] studied the influence of seven types of surface coating on ground and rough scaled solid clay units, i.e. steel plate, grind, plywood, hard-board, 6 layers of polythene, rubber with fibres, and pure rubber, reporting high strength differences depending on the bearing material. Page [6] studied in 1984 the influence of the birch plywood sheets in calcium silicate units, comparing with the unconfined units tested with brush platens. Khalaf et al. [43] studied different bearing surface treatments for masonry units in 1989, such as grinded, capped with cement mortar, plywood packing or using dental plaster in a polythene bag. Khalaf et al. [43] found that the grinded specimens were stronger than the other specimens, being the difference smaller for low or medium strength bricks. Khalaf et al. [43] recommended to test the solid brick specimens with grinded surfaces instead of considering capped ones, but packing was suggested to test the block specimens. Templeton et al. [44] studied the methods to prepare the bearing surfaces in 1990, as referred in the withdrawn of the ISO 9652-4 [45], i.e. grinding and capping with cement mortar, founding that the specimens capped with cement mortar offered lower compressive strength than the grinded ones. Page et al. [16], in 1991, studied the influence of the packing hollow concrete bricks using plywood or fibreboard, reporting a reduced experimental strength on specimens tested with fibreboard. Drysdale et al. [46] suggested in 1994 that masonry units can be tested using hard capping materials, such as sulphur mortar or gypsum plaster as indicated in the ASTM, and other capping materials, such as fibreboard, plywood or PTFE leaves, greased platens or brush platens. Drysdale et al. [46] evidenced that specimens tested with hard capped materials (gypsum plaster) produced higher experimental strengths, without establishing a relationship with those capped with soft materials like fibreboard. Crouch et al. [47] studied the use of the Neoprene pads in concrete masonry units in 1999, reporting a 20% reduction in strength for the specimens tested with Neoprene pads compared to those tested with gypsum cement caps, due to the excessive expansion of the Neoprene pads. In 2010, Lourenço et al. [48] recommended the use of oiled PTFE leaves to reduce the confinement while

testing solid fired clay bricks. In 2016, Aubert et al. [49] compared grinding with placing oiled leaves of PTFE on 50 mm cubic specimens of earth bricks, finding similar compressive strengths.

Murray [10], Daniel et al. [50], Neville [51] and Morsy [42] prevented the use of flexible materials from being applied on bearing surfaces. Murray [10], Daniel et al. [50] and Neville [51] indicated the importance of limiting the differences of Poisson's ratios between the bound material and the specimen. Murray [10] suggested that the most desirable conditions results from using capping materials that are as strong as the tested material and have similar modulus of elasticity and Poisson's ratio. Daniel et al. [50] reported that soft capping materials, such as lead and rubber, can deform outwards when the specimen is loaded producing radial stresses. Thus, soft materials such as Neoprene reduce the apparent compressive strength of the specimen, as previously observed by Richardson in concrete specimens [33] and Crouch et al. in concrete units [47]. The capping Neoprene can produce higher confinement in the centre of the specimen than in the borders, as analysed by Braga et al. [52]. Kleeman et al. [53] studied the mechanical properties of four different materials commonly used as packing material in compression tests on masonry, i.e. plywood, hardboard, fibreboard and particle board, concluding that the packing material's tangent moduli increase with increasing stress, and so does the tangent shear moduli. Morsy [42] concluded that flexible materials such as polyethylene (PE), rubber, or rubber with fibres tend to deform under the load application because of their Poisson's ratio higher than that of the clay material [54,55]. Schickert [18] compared the lateral strains and experimental strengths of the specimens tested with grinded surface, lubricated aluminium sheets, and steel brush platens, reporting that the specimens tested with aluminium sheets has 94% the strength of the specimens tested with rigid steel platens, and 81% the strength of the specimens tested with steel brushes. In addition, the lateral strain measured close to the bearing surfaces was about 50% of that measured at half height on specimens tested with brush platens, 45% on specimens tested with aluminium sheets, and 20% to 30% on specimens tested with steel platens. Schickert [18] considered that lubricated aluminium sheets produced more unrestrained deformation than steel platens, being close to that produced using the brush platens. The research group of RILEM TC 148-SSC [39] tested concrete specimens using PTFE leaves (single or double) and concluded that the strength and the pre-peak stress–strain behaviour became independent of the specimen slenderness.

International reference standards for masonry units recommend different surface treatments. The American ASTM C67-21 [56] for clay units recommends to cap the bearing surfaces with cement mortar, gypsum plaster or sulphur filler, while the ASTM C140/C140M-18 [57] for concrete and calcium silicate bricks specifies to cap the specimens with gypsum cement or sulphur filler following the ASTM C1552-16 [58]. The European EN 772-1+A1 [59] recommends to grind the surfaces or to cap them with cement mortar. The Australian AS/NZS 4456.4 [60] recommends the use of two sheets of 4 to 6 mm plywood, hardboard or 12 mm thick fibreboard. The Canadian CAN/CSA A82:14 (R2018) [61] indicates the use of gypsum plaster or sulphur filler to cap the bearing surfaces, while the CAN/CSA A165-14 (R2019) [62] refers to the American ASTM C140 [57].

A review of the American and European standards for concrete testing shows that the American ASTM C39-21 [63] recommends grinding, capping with high-strength gypsum or sulphur mortar following the ASTM C617-10 [64], or capping with Neoprene pads following the ASTM C1231/C1231M-14 [65], while the European EN 12390-03 [66] recommends grinding or capping with calcium aluminate cement, sulphur filler or iron sandbox.

This paper considers whole bricks, half bricks, 100×100 mm^2, and 40×40 mm^2 specimens for the experimental evaluation of the influence the cross section aspect ratio and the bearing surface treatment on the compressive strength of solid fired clay bricks. The analysed treatments considered are grinding, capping with cement mortar or gypsum plaster, placing birch plywood or medium density fibreboard (known as MDF). The interpretation of the experimental results is carried out according to a detailed analysis, quantifying the differences amongst the experimental strengths depending on the chosen approach. Additionally, this paper proposes the use of two novel bearing surface treatments to generate low boundary friction, i.e. covering with gypsum powder, and placing two oiled PTFE leaves. Few references have been found in the scientific literature about the use of gypsum powder related with the DIN 18555-9 [67] for testing mortar joints, e.g. Pelà et al. [68], while other studies used talcum powder as covering material in concrete, e.g. Ghadami et al. [69] and RILEM TC 148-SSC [39]. Several references recommend to use oiled PTFE leaves, such as RILEM TC 148-SSC [39] and Hussein et al. [17] for concrete, Lourenço et al. [48] for solid clay bricks, and Aubert et al. [49] for earth bricks. This paper considers the use of two oiled PTFE leaves on each bearing surface to reduce the friction between the press platen and the specimen's surface, in order to ensure a more uniform distribution of stresses. The use of two leaves reduces the radial stresses caused by the deformations of the PTFE in contact with the press platen due to the very low coefficient of friction (around 0.04, as indicated by the manufacturers). In addition, the additional use of mineral oil between both PTFE leaves ensures minimising further the friction of the system.

This research offers the results of an experimental campaign on two different solid fired clay brick types characterised by different manufacturing process, i.e. mechanically extruded and handmade, including the execution of 458 laboratory tests. The research encompasses the following specific objectives: (1) evaluating a methodology to estimate an equivalent compressive strength value in specimens that exhibit a hardening response in the experimental stress-displacement curve; (2) exploring the influence of the specimen's cross section aspect ratio on the determination of the compressive strength; (3) determining the influence of the bearing surface treatment on the experimental compressive strength; and (4) comparing four available reference standards with different recommendations about specimens' geometry and surface treatments for the experimental determination of the compressive strength.

The paper is structured in five sections. After this introduction, Section 2 presents the experimental campaign performed on solid fired clay bricks, including the description of the materials, the specimens' and bearing surfaces' preparation, and the testing procedure. Section 3 shows the experimental results. Section 4 analyses the experimental estimation of the equivalent compressive strength values for specimens with hardening response, the influence of the cross section's aspect ratio and of the different bearing surface treatments on the compressive strength, and the comparison of four different international standards for the determination of the compressive strength. The paper ends with Section 5 presenting some conclusions and future works.

2. Materials and testing method

This section presents the experimental campaign executed on solid fired clay bricks, both mechanically extruded and modern handmade, to study the effect of the specimen's cross section aspect ratio and the use of different bearing surface treatments on the compressive strength. Details are provided about the materials, the preparation of specimens and their bearing surfaces, and the testing setup. All experimental tests were carried out at the Laboratory of Technology of Structures and Materials of the Technical University of Catalonia (UPC-BarcelonaTech).

2.1. Materials

Two types of solid fired clay units were considered in this research (Fig. 1). The first type of unit, identified with the acronym 'Ex', corresponds to modern solid fired clay bricks produced by mechanical extrusion in an automated process. The automated process consists in mixing the raw material in a pug mill, and when the clay is uniform in

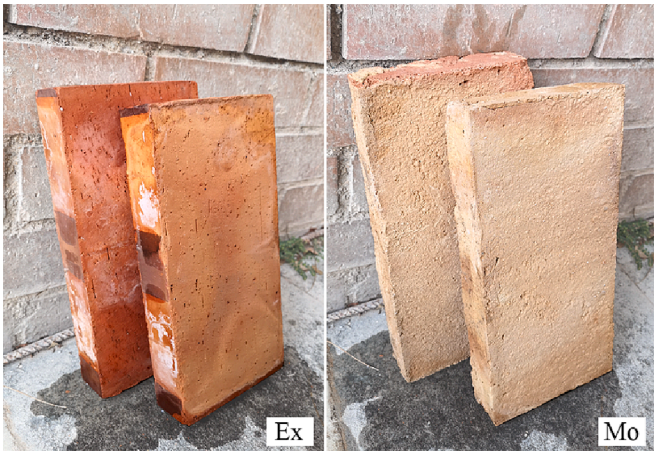

Fig. 1. Modern mechanically extruded solid fired clay brick (Ex) (left), modern handmade solid fired clay brick (Mo) (right).

consistency is put into the hopper of the extruder. The hopper puts the clay into the barrel of the extruder. Inside the barrel, a rotating screw moves the clay through a die, which is shaped like the bed-plane of the brick. The 'Ex' units are extruded perpendicular to the bed surface. As the extruded clay leaves the die, it is cut into the desired thickness by a wire cutter. The unit is then transported to a drying area, where it is dried before firing, loaded into a tunnel kiln, and fired with controlled heat conditions at 900 °C. The second type of unit, identified with the acronym 'Mo', corresponds to modern handmade solid fired clay bricks. 'Mo' units were traditionally manufactured in a brickyard by moulding. The raw material is mixed in a though and soaked in water for hours to soften it. The wet clay is shaped in a wooden mould sprinkled with dry fine sand. Then, the moulded clay brick is left to dry under the sun and, after extraction from the mould, they are fired into a coal-fired kiln at 950 °C.

The great availability of modern handmade (Mo) and extruded (Ex) units gave the possibility to test a larger number of specimens. Table 1 presents a description of the sampled materials in terms of origin, acronym, average dimensions measured according to EN 772-16 [70], net (ρ_{nu}) and gross (ρ_{gu}) dry density, open porosity (P_0), water absorption capacity (W_s), initial rate of water absorption ($C_{w,i}$), Young's modulus (E_b), and Poisson's ratio (ν_b). The net and gross dry density (ρ_{nu} and ρ_{gu}) were obtained according to EN 772-13 [71] and EN 772-3 [72], the open porosity (P_0) following the EN 772-4 [73], the water absorption (W_s) following EN 772-21 [74], and the initial rate of water absorption ($C_{w,i}$) following EN 772-11 [75]. The values of elastic modulus (E_b) and Poisson's ratio (ν_b) were determined following the testing procedures proposed in Makoond et al. [76].

2.2. Shape of specimens

The shape of specimens was determined by analysing the available standards and the literature in the field. A total of four shapes for specimens was proposed, i.e. the whole brick identified as '*wh*', the half brick identified as '*ha*', the cut specimens with cross section measuring 100 × 100 mm^2 identified as '*100*' and 40 × 40 mm^2 identified as '*C40*'. The proposed whole brick '*wh*' is recommended by the AS/NZS 4456.4 [60], CAN/CSA A82:14 (R2018) [61], IS 3495-1:2002 [77] and RILEM recommendation LUMA.1 [78]. The proposed half brick '*ha*' is recommended by the ASTM C67-21 [56] by using a specimen with the full height and width of the original brick, and the length equal to one half of the full brick's length. The '*ha*' is also allowed by AS/NZS 4456.4 [60] and CAN/CSA A82:14 (R2018) [61] as long as the unit is symmetrical and the whole brick exceeds the capacity of the testing machine. The 100 × 100 mm^2 specimen '*100*' is included in the EN 772-1 + A1:2016 [59], and in the withdrawn of the ISO 9652-4 [45]. The EN 772-1 +

Table 1
Classification of tested units in terms of origin, acronym (Acr.), average dimensions, net and gross dry density, open porosity, water absorption capacity, initial rate of water absorption, Young's modulus, and Poisson's ratio. Values in brackets correspond to the coefficients of variation (CV).

Sampled materials											
Origin	Acr.	Av. Dimensions (mm)			ρ_{nu} (kg/m^3)	ρ_{gu} (kg/m^3)	P_0 (%)	W_s (%)		$C_{w,i}$ (kg/(m^2 × min))	E_b (GPa)	ν_b [-]
		EN 772–16			EN 772–13		EN 772–4	EN 772–21		EN 772–11	Makoond et al. [76]	
Mechanically extruded	Ex	272 [0.4%] × 132 [0.9%] × 45 [0.7%]			1529 [5.5%]	1677 [0.8%]	26.7 [5.7%]	17.5 [1.9%]	length	0.0405 [7.8%]	13.0 [15.1%]	0.20 [44%]
									width	0.0374 [9.4%]	11.5 [15.5%]	0.13 [43%]
Modern handmade	Mo	311 [0.6%] × 149 [1.7%] × 46 [4.6%]			1631 [5.6%]	1761 [1.2%]	25.5 [7.0%]	15.7 [7.0%]	length	0.0322 [20.1%]	6.3 [28.8%]	0.12 [49%]
									width	0.0316 [23.0%]	5.6 [24.0%]	0.10 [57%]

A1:2016 [59] does not specify the size of the specimen to be tested. However, it indicates the possibility of testing representative portions cut from the whole unit. The EN 772-1 + A1 does not indicate explicitly the need to test a square cross section sample, and its Table A.1 indicates only the width as reference parameter to evaluate the so-called "shape factors" accounting for the dimensions of the specimen. For a specimen with height below 50 mm, the standard EN 772-1 + A1 only allows a width value ranging from 50 mm to 100 mm. Therefore, the proposed '*100*' specimen satisfies the European standard requirements. The 40 × 40 mm^2 specimen '*C40*' was adopted by Cabané et al. [4] as a specimen of slenderness equal to one.

In addition, to analyse the effect of the cross section aspect ratio, stacked '*wh*' and '*ha*' specimens were made up, according with the EN 772-1 + A1 [59] recommendation, placing one grinded specimen upon another grinded one, without any intermediate material. Thus, two types of stacked specimens were proposed, i.e. the stacked whole brick identified as '2*wh*', and the stacked half brick identified as '2*ha*'.

A total amount of 458 specimens were prepared and tested, including 111 '*wh*', 97 '*ha*', 114 '*100*', 98 '*C40*', 20 '2*wh*', and 18 '2*ha*' specimens.

2.3. Treatments of the bearing surfaces of specimens

The specimens were prepared following a controlled procedure. First, the bricks were cut using a table saw equipped with a water jet to obtain '*ha*', '*100*' and '*C40*'. The '*100*' and '*C40*' specimens were obtained from the central parts of the bricks. Then, the specimens were dried in an oven at a constant temperature of 105 ± 5 °C for 24 h. Finally, the specimens' dimensions were measured before preparing the bearing surfaces using a calliper with an accuracy of ±0.1 mm according to EN 772-16 [70]. The specimens with grinded surfaces were also measured after the grinded process.

Different bearing surface treatments were considered, as explained in Section 1, based on the available international standards for masonry clay units, the RILEM LUMA.1 recommendations, the ISO 9652-4 withdrawn, and the scientific literature, i.e. grinding [45,59,78], capping with cement mortar [45,56,59,78], capping with rapid-setting industrial gypsum plaster [56,61,77], inserting a sheet of plywood [60], and inserting a sheet of fibreboard [60]. Capping with sulphur-filler [56,61,77] was not considered in this research for environmental and health issues as warned in the ASTM C1552-16 [58]. Another reason is that specimens capped with sulphur-filled exhibited similar compressive strength than those capped with cement mortar in previous research on concrete specimens [79,80]. The use of unbonded Neoprene pads [63] was also not considered in this research because its use has been highly questioned [10,42,47,50,51,81]. Instead, two other novel testing procedures were proposed in this research to reduce the friction effect, i.e. covering with gypsum powder, and inserting two oiled leaves of PTFE. The covering of the bearing surfaces with gypsum powder provided smoothing to the rough surfaces of the specimen, while the small diameter of the powder particles guaranteed reduced friction. The insertion of two oiled PTFE leaves was recommended by RILEM TC 148-SSC [39] to test concrete specimens, an also by Lourenço et al. [48] to test clay bricks.

To summarise, the considered treatments for the specimens' bearing surfaces were (1) grinding, (2) capping with cement mortar, (3) capping with gypsum plaster, (4) inserting a sheet of birch plywood, (5) inserting a fibreboard sheet, (6) covering with gypsum powder, and (7) inserting two oiled leaves of PTFE. Fig. 2 shows the specimens with the different bearing surface treatments considered in this research. Different materials and procedures were followed in the laboratory to prepare the bearing surfaces.

(1) To grind the surfaces, a grinder fitted with a high speed rotating diamond disc was used until the requirements for flatness and parallelism were achieved. After the grinding process, the remaining height of the samples was 40 mm. The remaining height of the samples was conditioned by the original height of the bricks (with raw thickness ranging between 44 mm and 48 mm). Handmade (Mo) bricks required a greater reduction of the original thickness than the mechanically extruded (Ex) units due to irregularities in the solid clay beds.

(2) To cap the surfaces with cement mortar, a composed mortar of 1 part of cement CEM II/A-L 42,5R and 3 parts of sand was used with a maximum grain size of 2 mm. Additionally, silica fume was used in 5% by weight of cement to increase the cap's compressive strength [82]. The mixture was made having a water-to-cement ratio of 0.50 and adding a water reducer [82]. The capping procedure was executed on a wooden plate coated with a film of oil, and a spirit level to ensure the specimen's horizontality. The time between capping one bearing surface and the other was 24 h.

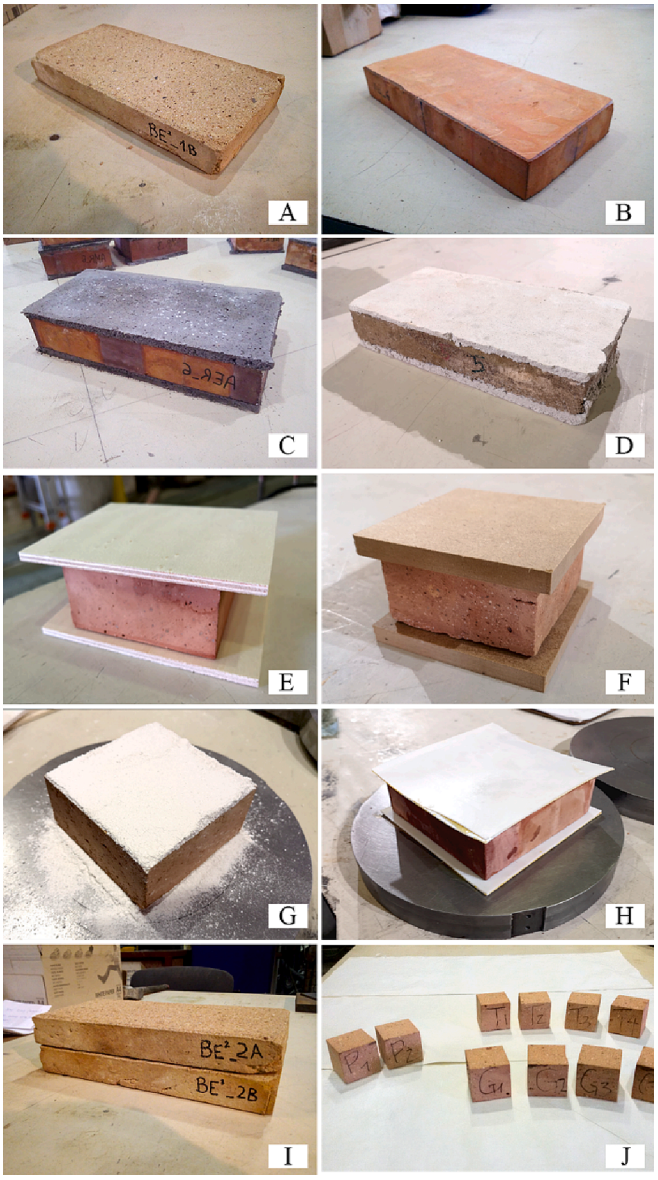

Fig. 2. The considered bearing surface treatments for compressive testing. (A) Whole handmade brick with grinded surfaces. (B) Whole mechanically extruded brick with grinded surfaces. (C) Whole brick with cement mortar capped surfaces. (D) Whole brick capped with gypsum plaster. (E) '*100*' specimen with a sheet of 5 mm ply birch plywood. (F) '*100*' specimen with a sheet of 12 mm fibreboard (MDF). (G) '*100*' specimen covered with gypsum powder. (H) Half brick with a leaf of PTFE. (I) Stacked specimen composed of 2 grinded whole bricks. (J) '*C40*' specimens with grinded surfaces.

After the second surface was capped, the specimens were aged 28 days before testing in laboratory conditions. The thickness of each cap was approximately 5 mm. The mortar's compressive strength (f_m) of 56.5 MPa (CV 16%) and the bending strength ($f_{flex,m}$) of 7.3 MPa (CV 16%) were evaluated according to EN 1015–11 + A1 [83] by using 160 × 40 × 40 mm^3 prisms casted with the same material employed during the construction of the capped specimens.

(3) To cap the surfaces with gypsum plaster, a rapid-setting industrial gypsum was used. The mixture was made having a water-to-gypsum ratio of 0.5 l for each kg. The capping procedure was executed on a wooden plate coated with a film of oil, and a spirit level to ensure the specimen's horizontality. Before capping the specimens with gypsum, the surfaces were cleaned from dust, and coated with shellac to allow them to dry thoroughly. The shellac was applied with a conventional low-pressure spray gun. The time between capping one bearing surface and the other was 1 h. After the second surface was capped, the specimens were aged 24 h before testing in laboratory conditions. The thickness of each cap was approximately 5 mm. The gypsum's compressive strength (f_{gy}) of 5.7 MPa (CV 7.7%) and the bending strength ($f_{flex,m}$) of 2.2 MPa (CV 7.8%) were evaluated according to EN 1015–11 + A1 [83] by using 160 × 40 × 40 mm^3 prisms casted with the same material employed during the construction of the capped specimens.

(4) Two 5 mm thick plywood sheets were placed on top and bottom of the brick specimens. The 5 mm ply birch plywood had a longitudinal and transverse flexural strength of 82 MPa and 32 MPa, a longitudinal and transverse modulus of elasticity of 11 GPa and 6.6 GPa respectively, and a tensile strength along the fibres greater than 30 MPa. The length and width of the plywood sheets exceeded the specimens' dimensions by 10 mm to 30 mm.

(5) Two 12 mm thick fibreboard sheets were placed on top and bottom of the brick specimens. The 12 mm medium density fibreboard (MDF) had a flexural strength of 30 MPa, a tensile strength of 0.60 MPa, and a modulus of elasticity of 2.5 GPa. The length and width of the fibreboard exceeded each specimens' dimensions by 10 mm.

(6) To cover with gypsum powder, a thin uniform coat was used of dry powder gypsum with a grain size less than 1 mm. The lower powder coating was placed on a metal plate with a gypsum thickness of approximately 5 mm. Then, the specimen was pressed firmly onto this layer, ensuring its horizontality with a spirit level. Finally, the upper powder coating with a thickness equal to the lower one was placed on the specimen and covered with a second metal plate.

(7) The treatment with two 1 mm thick oiled PTFE leaves placed on the top, and two other placed on the bottom of the brick specimens. The treatment previously includes the grinding of the specimen surfaces as specified in point (1). The mineral oil applied by brush had a viscosity index of 150. The length and width of the PTFE leaves exceeded the corresponding specimens' dimensions by 10 mm.

2.4. Testing procedures

The specimens were tested making use of two different testing machines with different loading capacity depending on the specimen's expected compressive strength. The Ibertest testing machine was equipped with three different load cell, 3000 kN (MEH-3000), 200 kN, and 10 kN (AUTOTEST 200/10 SW), and connected to a MD5 electronic module for data acquisition. The Ibertest AUTOTEST 200/10 SW was used for bending and compressive tests of the 160 × 40 × 40 mm^3 cement mortar and gypsum plaster capping material, and to test the specimens '*C40*'. The Ibertest MEH-3000 was used to test all specimens except mechanically extruded ('Ex') whole brick '*wh*'. The Suzpecar testing machine was equipped with a load cell of 5000 kN and connected to a FlexTest60 controller. All the 'Ex' whole bricks '*wh*' were tested in the Suzpecar testing machine, regardless of the bearing surface treatment due to the need for loads greater than 3000 kN.

The specimens were centred on the steel plates with the bearing surfaces orthogonal to the direction of the loading. The specimens in the Ibertest machine were tested under force control, and the specimens in the Suzpecar machine were tested under force control until one-half of the expected maximum load and then under strain control. The application of the load was selected in order to meet the requirements of the reference standards. The AS/NZS 4456.4 [60] allows a constant load application under force control between 0.15 MPa/s and 0.70 MPa/s, or under strain control between 1 and 5 mm/min without specifying a minimum test duration. The IS 3495–1:2002 [77] also indicates a constant load application of 0.23 MPa/s. The CAN/CSA A82:14 (R2018) [61] and ASTM C67-21 [56] recommends that the duration of the second half of the expected maximum load be between 60 and 120 s, without specifying a constant load application. The EN 772-1 + A1:2016 [59] recommends that the duration of the second half of the expected maximum load be over 60 s, offering an indicative table of load application between 0.05 MPa/s and 1.00 MPa/s. Thus, the specimens in the Ibertest machine were tested at 0.15 MPa/s, 0.30 MPa/s or 0.60 MPa/s rates depending on the specimen capacity to comply with all standards referenced in this research, and to guarantee that the second half of the expected maximum load be between 60 s and 120 s. The specimens in the Suzpecar machine were tested at a rate of 0.30 MPa/s until reaching the half of the expected maximum load, and then under strain control at a rate of 1 mm/min.

The tests were stopped manually after registering the post-peak response of the force–displacement pattern. The specimens that showed a strain-hardening response, as explained in Section 3.2, were stopped after 120 s ensuring all slope changes in the stress-displacement response.

3. Experimental results

This section presents the experimental results of compressive strength in solid fired clay brick specimens with different cross-section aspect ratio and different bearing surface treatments. First, details are given about the experimental average values of compressive strength and their coefficients of variation (CV), the number of specimens, the analysis of the stress-displacement graphs, and the description of the specimens' failure modes. Second, various methods are analysed for estimating an equivalent compressive strength in specimens that exhibit a hardening response.

3.1. Results derived from compression tests

Table 2 presents the number of specimens for each proposed treatment of the bearing surfaces, with their average compressive strength (f_c), and coefficients of variations (CV). The compressive strength of the samples was calculated by dividing the maximum compressive load by the cross-sectional area of the specimen. The displacement during the test was measured with the transducer from the actuator.

The 'Ex' '*wh*' and '*ha*' specimens showed similar compressive strengths for grinded, capped with cement mortar, capped with gypsum plaster, and placed with fibreboard sheets. The 'Mo' '*wh*' and '*ha*' grinded, capped with gypsum plaster, and covered with gypsum powder showed a hardening response without a maximum in the stress-displacement curve, and thus they required a careful post-processing analysis to propose an equivalent compressive strength value, see Section 3.2. The 'Mo' '*100*' and '*C40*' capped with gypsum plaster showed similar strengths. In both 'Ex' and 'Mo' types, the grinded specimens showed the highest average strength while those capped with gypsum plaster showed the lowest results. The '*C40*' placed with plywood or fibreboard sheets showed the highest strength, while '*C40*' covered with

Table 2
Number (N) and average compressive strength (f_c) of the tested specimens with different bearing surfaces treatments and cross section aspect ratio. Values in brackets correspond to the Coefficients of Variation (CV). (width maximum 19 cm).

Tested specimen															
Origin			Grinded		Cement Mortar Capped		Gypsum Plaster Capped		Birch Plywood Sheets		Fibreboard Sheets		Gypsum Powder Covered		Oiled PTFE leaves	
			N	f_c (MPa)	N	f_c (MPa)	N	f_c (MPa)	N	f_c (MPa)	N	f_c (MPa)	N	f_c (MPa)	N	f_c (MPa)
Ex	'*wh*'		10	90.0 [1.6%]	12	77.3 [7%]	8	63.8 [7%]	6	89.4 [2.2%]	6	76.7 [2.5%]	8	84.5 [8%]	6	29.9 [5%]
	'*ha*'		6	88.1 [4%]	6	81.9 [3%]	8	68.0 [7%]	6	77.0 [3%]	6	72.9 [5%]	6	73.8 [10%]	6	34.0 [7%]
	'*100*'		6	75.3 [3%]	6	59.3 [19%]	8	55.2 [7%]	6	75.2 [2.3%]	6	71.7 [2.2%]	6	66.4 [5%]	6	36.9 [6%]
	'*C40*'		12	51.1 [14%]	6	37.8 [26%]	6	29.7 [11%]	6	65.4 [11%]	6	68.2 [4%]	6	24.4 [10%]	6	36.4 [8%]
	'*2wh*'		8	57.7 [8%]	–	–	–	–	–	–	–	–	–	–	–	–
	'*2ha*'		6	59.6 [10%]	–	–	–	–	–	–	–	–	–	–	–	–
Mo	'*wh*'	Point (2) secant slope	9	29.6 [10%]	14	33.0 [15%]	8	24.8 [15%]	6	41.0 [16%]	6	36.7 [7%]	6	27.8 [10%]	6	10.3 [11%]
		Point (3) 2nd der.max.		35.3 [14%]				24.5 [25%]						27.2 [13%]		
		Point (4) 2nd der. 0		43.4 [9%]				27.1 [20%]						32.7 [19%]		
	'*ha*'	Point (2) secant slope	7	23.2 [20%]	16	25.1 [10%]	6	13.6 [9%]	6	27.2 [12%]	6	27.1 [7%]	6	20.7 [9%]	6	11.0 [20%]
		Point (3) 2nd der.max.		31.4 [14%]				16.1 [15%]						22.1 [10%]		
		Point (4) 2nd der. 0		33.0 [13%]				17.4 [12%]						25.0 [9%]		
	'*100*'		14	24.9 [8%]	10	20.2 [7%]	22	10.4 [14%]	6	23.8 [19%]	6	22.4 [8%]	6	15.9 [15%]	6	9.3 [19%]
	'*C40*'		6	11.5 [15%]	8	11.7 [23%]	8	10.7 [24%]	6	14.5 [29%]	6	17.8 [11%]	8	4.6 [22%]	8	8.0 [16%]
	'*2wh*'		12	22.7 [20%]	–	–	–	–	–	–	–	–	–	–	–	–
	'*2ha*'		12	17.8 [12%]	–	–	–	–	–	–	–	–	–	–	–	–

gypsum powder showed the lowest strength, even lower than the specimens tested with oiled PTFE leaves. The strengths obtained on the specimens tested with oiled PTFE leaves are similar for different specimens' cross sections within the respective 'Ex' and 'Mo' types of unit. The influence of specimen's length and bearing surface treatment on the compressive strength is presented in Section 4.

The CV ranged between 1.6%–26% for mechanically extruded ('Ex') units, and between 7%–29% for modern handmade ('Mo') units. The 'Ex' bricks exhibited higher average compressive strength and a general lower CV than the 'Mo' bricks. The higher CV in 'Mo' units is due to the larger inhomogeneity of the bricks, as well as to their non-industrialised manufacturing. In addition, slightly lower CV values were obtained in 'Ex' grinded units, and the highest CV values were obtained in the 'Mo' specimens capped with gypsum plaster.

Fig. 3 shows the stress-displacement curves of the '*wh*', '*ha*', '*100*' and '*C40*' samples of the mechanically extruded (Ex) and modern handmade (Mo) bricks with the different treatments of the bearing surfaces. The stress-displacement curves with different bearing surfaces yield significantly different experimental stiffness depending on the bearing surface treatment, being much more evident in the 'Mo' specimens.

The tested specimens exhibited two main different responses. On one hand, a strain-hardening response due to a confinement effect was observed in the 'Mo' '*wh*' and '*ha*' grinded, capped with gypsum plaster and covered with gypsum powder, producing a continuous increasing of stress and deformation. On the other hand, a softening post-peak response was observed in the other specimens. The determination of the compressive strength in the specimens exhibiting hardening may be hindered by the fact that a full failure may not be obtained. Specimens can maintain their load-bearing capacity due to triaxial confinement, and withstand very high levels of compression, despite undergoing a complete physical transformation involving a total loss of cohesion. Therefore, an estimation of an equivalent compressive strength could be associated with the level of compression for which the physical transformation occurs. To overcome this problem, a mathematical analysis is proposed in Section 3.2 to determine a slope change in the stress-displacement response. Strain-hardening responses are also discussed in detail in Section 4.1.

In addition, different responses are obtained depending on the specimen's bearing surface treatment. The curves of the specimens grinded, and capped with cement mortar are either overlapped or parallel, showing very similar stiffness that is the highest one amongst those derived from all the treatments. The curves of the specimens capped with gypsum plaster show a similar initial behaviour and stiffness than the grinded and capped with cement mortar, however the displacements during the test were strongly influenced by the size of the sample. The curves of the specimens 'Ex' with plywood sheets show a low initial stiffness. This behaviour may be related with the fact that the plywood is compressed and adapts to the specimen surface. After this initial behaviour, the curves exhibit increasing stiffness with approximately linear branch up to the strength. In addition, the 'Mo' specimens with plywood show lower stiffness in the final part of their stress-displacement response. The curves of the specimens tested with fibreboard show a rather constant stiffness up to the specimen strength. However, the curves of the 'Ex' '*wh*' and '*ha*' specimens show some irregularities in the stress-displacement response starting from 70 MPa.

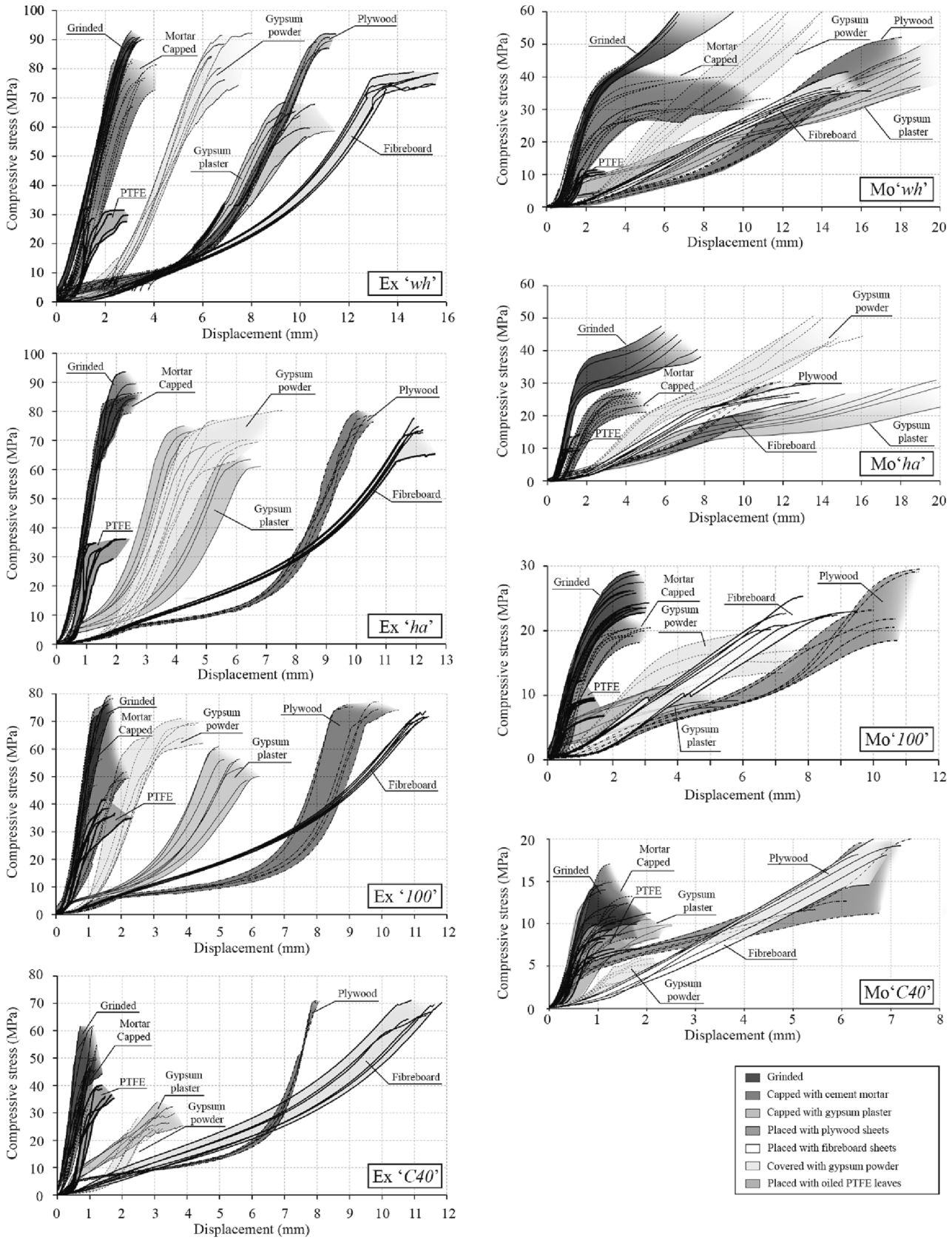

Fig. 3. Stress-displacement curves of the mechanically extruded (Ex) and of the modern handmade (Mo) of '*wh*', '*ha*', '*100*' and '*C40*' specimens under compression with different treatments for the bearing surfaces.

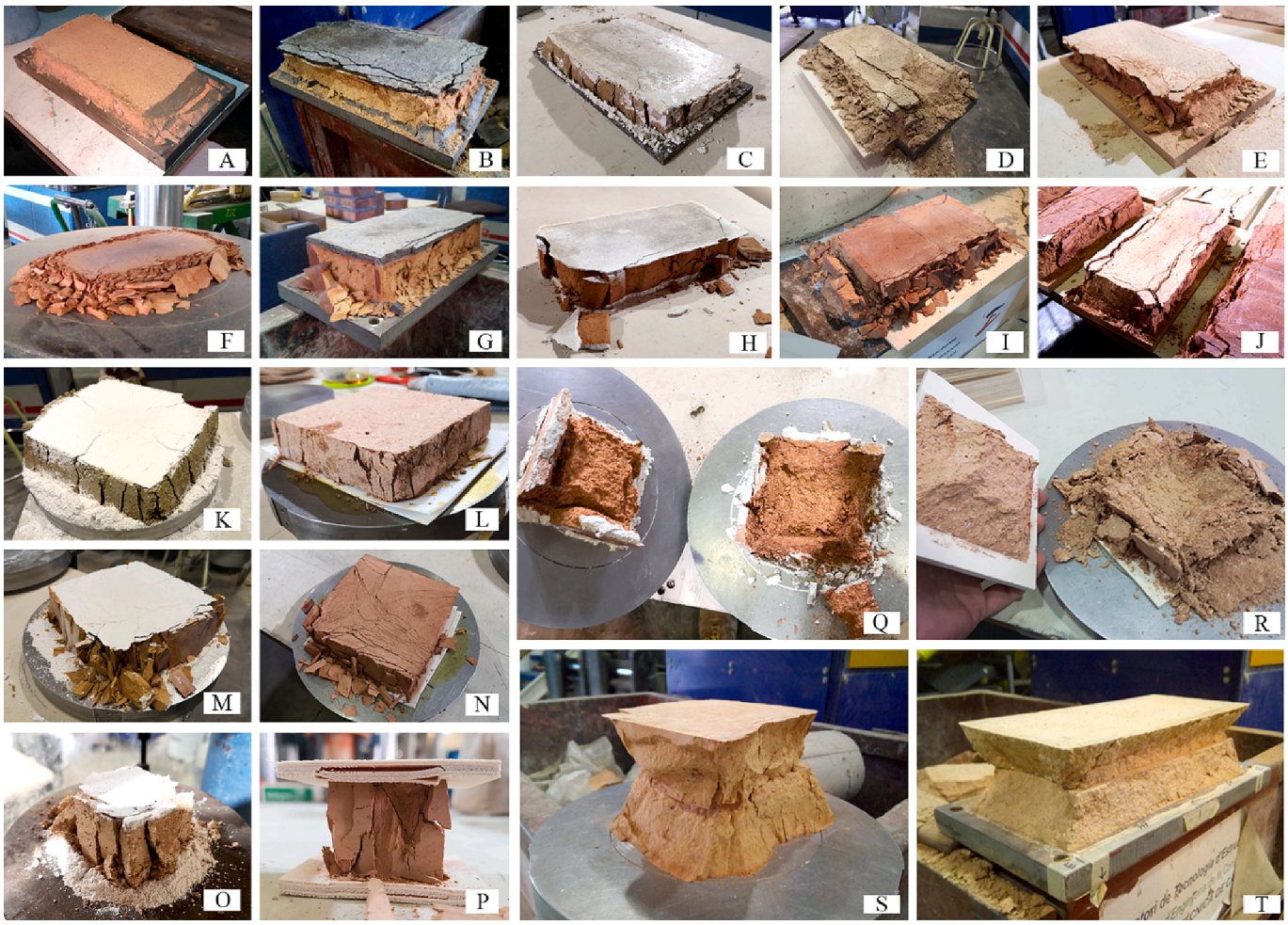

Fig. 4. Observed failure modes in the specimens with all bearing surface types. Handmade bricks 'Mo' from (A) to (E), (K), (L), (O), (Q), and (R). Mechanically extruded bricks 'Ex' from (F) to (J), (M), (N), (P), (S), and (T). (A) and (F) grinded, (B) and (G) capped with cement mortar, (C) and (H) capped with gypsum plaster, (D) and (I) placed with sheets of plywood, (E) and (J) placed with sheets of fibreboard, (K) and (M) covered with gypsum powder, (L) and (N) placed with two oiled PTFE leaves. (O) 'Mo' '*C40*' covered with gypsum powder, (P) 'Ex' '*C40*' placed with sheets of plywood, (Q) 'Mo' '*100*' capped with gypsum plaster, (R) 'Mo' '*100*' placed with plywood sheets, (S) Ex '*2ha*' grinded and stacked. (T) Mo '*2wh*' grinded and stacked.

This change in behaviour can be influenced by the tensile failure of the fibreboard following the specimen failure crack pattern. The curves of the specimens tested with gypsum powder show a similar behaviour to that of specimens with gypsum plaster. The curves of the specimens tested with two oiled PTFE leaves show a behaviour similar to that of the specimens grinded and capped with cement mortar, although they reach much lower values of strength and maximum displacement.

3.2. Experimental failure modes

Regarding the observed experimental failure modes, all non-stacked specimens exhibited splitting and separation of the outer parts (Fig. 4a–t), while stacked specimens showed the typical hourglass (Fig. 4s and t). Handmade (Mo) '*100*' and '*C40*' specimens, after removing the split outer parts, also showed the hourglass failure. The '*100*' capped with gypsum plaster (Fig. 4q), and '*100*' and '*C40*' with plywood sheets (Fig. 4r) could be divided into two superimposed square frusta of pyramid at the end of the tests.

An in-depth evaluation of the experimental evidence allowed the detection of some differences in the failures modes, depending mainly on the surface treatment. The mechanically extruded units (Ex) with grinded surfaces (Fig. 4f), with plywood sheets (Fig. 4i and p), and with fibreboard (Fig. 4j) presented a brittle response with multiple vertical cracks appearing on the edges. The 'Ex' '*wh*' specimens with fibreboard sheets exhibited a sudden and noisy failure with detachment of material. The 'Ex' specimens capped with mortar (Fig. 4g), with gypsum plaster (Fig. 4h) and covered with gypsum powder (Fig. 4m) presented a brittle response with spaced vertical cracks. The 'Ex' specimens with oiled PTFE leaves (Fig. 4n) showed fragmentation of the brick material evenly distributed throughout the specimen [84–86]. The 'Mo' '*wh*' and '*ha*' with grinded surfaces (Fig. 4a), capped with gypsum plaster (Fig. 4c) and covered with gypsum powder (Fig. 4k) showed the expulsion of the outer material while the specimen's core remained compact without material cohesion, as will be also highlighted in Section 4.1. The 'Mo' specimens capped with cement mortar (Fig. 4b) or gypsum plaster (Fig. 4c) and covered with gypsum powder (Fig. 4k and o) presented also splitting of the outer parts with spaced vertical cracks. The 'Mo' specimens tested with plywood sheets (Fig. 4d), and with fibreboard (Fig. 4e) presented a total loss of cohesion of the perimeter as well as material expulsion. The 'Mo' specimens with oiled PTFE leaves (Fig. 4l) showed multiple vertical cracks evenly distributed throughout the edges of the specimen, with consequent loss of material cohesion.

A careful visual evaluation of the material interposed between the specimen and the press platens was executed after the tests. The cement mortar cap (Fig. 4b and g) showed a splitting failure according to an elliptical pattern close to the specimen's edges. The gypsum plaster (Fig. 4c and h) and the gypsum powder (Fig. 4k and m) appeared like a brittle thin sheet that could be easily separated from the 'Ex' specimens.

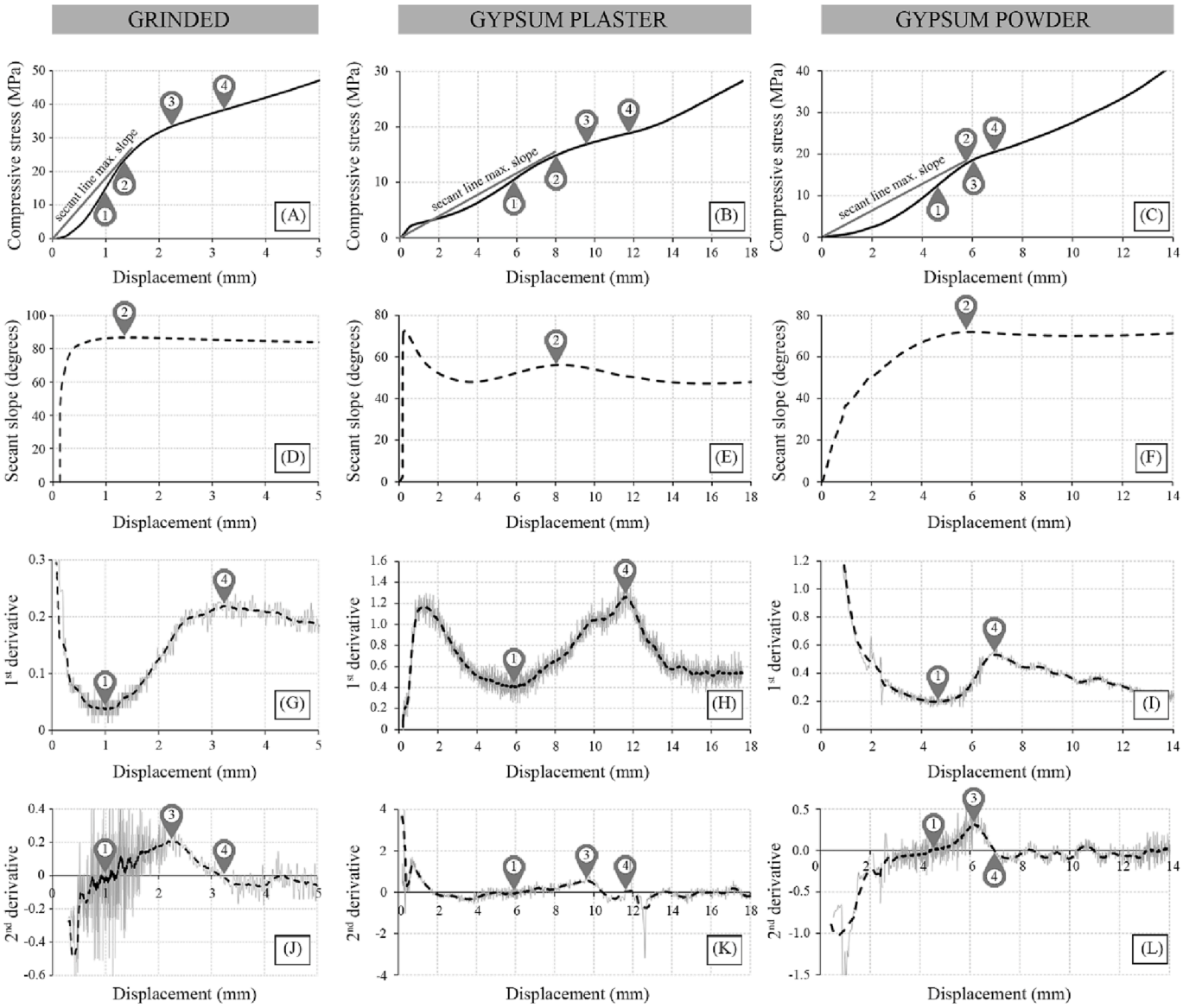

Fig. 5. (A), (B) and (C) Experimental stress-displacement curves of representative specimens with hardening response obtained from handmade bricks (Mo) with surfaces grinded, capped with gypsum plaster and covered with gypsum powder. The marked points correspond to the point of the maximum secant slope (point 2), the inflexion points of the stress-displacement curve (point 1 and 4), and the inflexion point of the 1st derivative function (point 3). (D), (E) and (F) show the slope of the secant line that intersects the origin and the stress-displacement curve, evidencing the local maximum (point 2). (G), (H) and (I) show the 1st derivative evidencing the local maximum (point 4) and the local minimum (point 1). (J), (K) and (L) show the 2nd derivative evidencing the local maximum (point 3) and the considered points with zero value (points 1 and 4).

The gypsum plaster and gypsum powder were stuck into the specimens' clay after the test, being impossible to peel off from the sample. The plywood sheets (Fig. 4d and i) were flattened over the specimen zone and presented the same crack patterns of the '*wh*' and '*ha*' specimen's beds, being either partially or completely embedded in '*100*' (Fig. 4r) and '*C40*' specimens (Fig. 4p) respectively. The fibreboard sheets (Fig. 4e and j) presented the same pattern as that explained for plywood at the end of the tests. The PTFE leaves (Fig. 4l and n) did not show any deformation in 'Mo' specimens. However, the PTFE leaves showed the imprint of the 'Ex' specimens' fragmentation on their surfaces.

3.3. Specimens with hardening response

As explained in Section 3.1, the 'Mo' '*wh*' and '*ha*' specimens with grinded surfaces, capped with gypsum plaster and covered with gypsum powder exhibited a hardening stress-displacement response. Since this peculiar behaviour does not allow one to identify unambiguously the compressive strength, this research proposes a novel method to estimate an equivalent compressive strength based on the identification of a representative point in the experimental stress-displacement response. Fig. 5a, b and c show the experimental stress-displacement curves of a representative specimen obtained from testing a '*wh*' grinded specimen (Fig. 5a), and from testing a '*ha*' capped specimen with gypsum plaster (Fig. 5b) or gypsum powder (Fig. 5c). The curves corresponding to specimens with grinded surfaces (Fig. 5a) and covered with gypsum powder (Fig. 5c) exhibit increasing stiffness at lower stress levels, which are related with the adjustment of the platens to the bearing surfaces of the specimens. However, the curves of specimens capped with gypsum plaster (Fig. 5b) start with a high stiffness response, which progressively decreases probably due to the deformation of the gypsum plaster. After this common initial stage, all the curves present an inflexion point. After the first inflexion point, denoted as point 1, the stiffness decreases until

reaching a second inflexion point, denoted as point 4, where the stiffness starts to increase until the loading is stopped at the end of the test. The inflexion points in the curves can be detected as the points with value zero in of the 2nd derivative (Fig. 5j, k and l).

In order to approximate the estimation of the compressive strength in these specimens, four mathematical criteria are proposed to identify four significant points: the point of the maximum secant slope (point 2), the inflexion points of the stress-displacement curve (points 1 and 4), and the inflexion point of the 1st derivative function (point 3). The point of the maximum secant slope (point 2) is determined by the maximum slope of the line that intersects the origin of the function and the stress-displacement curve. Since the curve of the specimens capped with gypsum plaster (Fig. 5b) shows an initial stage with high stiffness, the considered point 2 was the second relative maximum of the secant slope-displacement curve (Fig. 5e). Fig. 5d, e and f show the graphs indicating the secant slope vs. displacement curve evidencing the points 2. The inflexion points of the stress-displacement curve are determined by the relative maximum (point 4) and the relative minimum (point 1) of the 1st derivative function, see Fig. 5g, h and i, as well as by the zero values of the 2nd derivative function, see Fig. 5j, k and l. The inflexion point of the 1st derivative is determined by the relative maximum of the 2nd derivative (point 3). Fig. 5j, k and l shows the 2nd derivative evidencing the relative maximum (point 3) in the graph.

The four options aforementioned indicate "representative points" in the experimental stress-displacement response that might be considered to evaluate the compressive strength in specimens exhibiting a hardening response. Section 4.1 reports a comparative analysis amongst the different representative points.

4. Discussion

This section presents four analytical studies based on the experimental results described in Section 3. The first study analysed the proposed method to estimate an equivalent compressive strength on specimens with hardening response. The second study focuses on the influence of the cross section's aspect ratio on the resulting experimental compressive strength. The third study is aimed to understand the relationship between the compressive strength of the specimens and the bearing surface treatment. The fourth study analyses the different approaches available for the evaluation of the compressive strength, according to different available reference standards. The second and third study considers additional experimental data from the available literature in the field to complement those derived from the present experimental campaign.

4.1. Evaluation of the compressive strength in specimens with hardening response

Section 3.2 has highlighted the hardening response detected in 'Mo' '*wh*' and '*ha*' specimens with bearing surface grinded, capped with gypsum plaster and covered with gypsum powder, observing that it is possible to evaluate four "representative points" derived from a simple mathematical study of the stress-displacement experimental functions. This Section presents a careful analysis of the levels of damage reached in the tested specimens at each proposed point, to identify the most adequate value of the compressive strength.

The approach for evaluating the geometric macroscopic damage on the specimens follows the descriptions for concrete of Stroeven [87] and Kotsovos [88,89]. Stroeven [87] described an initial damage stage as discontinuous and gradual, observing an increasing of crack length and number, and a second stage consisting mainly of the union of the previous cracks. Kotsovos [88,89] described four damage stages. First, initial isolated microcracks appear and remain stable. Second, the initial microcracks begin to branch out in the direction of maximum principal compressive stress. Third, branching cracks start to propagate by spreading relatively steadily. Fourth, the crack pattern becomes unstable and failure occurs, marked by a rapid increase within the total volume of the material. Fig. 6 shows the stress-displacement curves of the representative specimens, indicating the four representative points and the relevant specimens' levels of damage. In addition to the specimens with hardening already presented in Section 3.2, the figure presents also two specimens with plywood sheets and with two oiled PTFE leaves as they also exhibited post-peak response with no clear compressive strength value. Fig. 6 shows the corner of the specimens to visualize two lateral edges. At point (1) the specimens began to show some diffuse and minor vertical cracking. At point (2) the specimens exhibited major

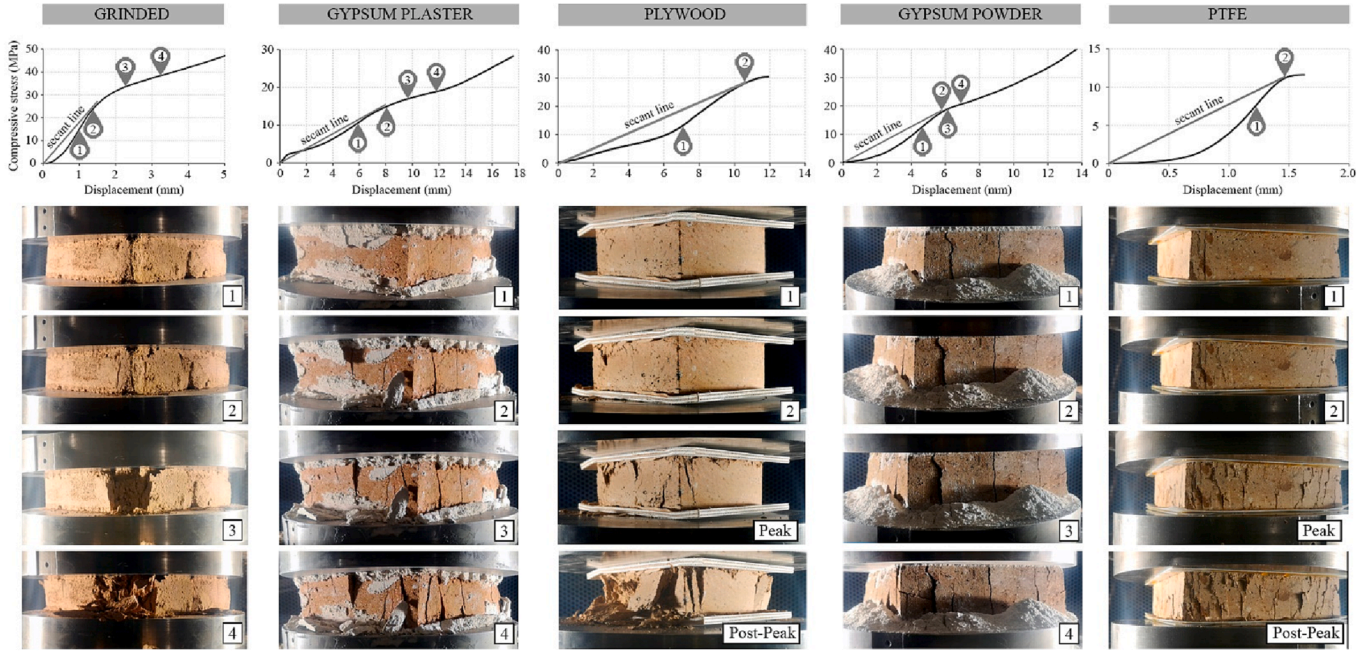

Fig. 6. Stress-displacement curves with hardening response for '*wh*' and '*ha*' specimens obtained from handmade bricks (Mo) for different bearing surfaces treatments, with levels of damage corresponding to the proposed representative points.

vertical cracking. At point (3) the main cracks widened and new vertical cracks emerged. At point (4) all the cracks widened and the specimen exhibited important lateral expansion, until the expansion stabilised causing a final increase of stiffness in stress-displacement curve until the test stopped. In the specimens with plywood sheets and with two oiled PTFE leaves, the considered points 1 and 2 can be obtained before reaching the peak or ultimate stress, when all the cracks connect and widen, and lateral expansion occurs in the post-peak.

The initial microstructure of the solid fired clay bricks depends of the firing temperature and the raw clay quality, where mineralogical and complex chemical reaction influence the brick material porosity, as explained by Fernandes et al. [90]. This porosity is related with the volume of void spaces in the material's microstructure. Fernandes et al. [91] reported that most common porosity in handmade solid fired clay bricks range between 25 and 35 vol%. Krakowiak et al. [86] analysed the microstructure of the mechanically extruded solid fired clay bricks reporting that the size of the particles varies depending on mineralogy of raw material and processing conditions. During the linear range, the material microstructure presents resistance against the splitting of the bonded particles. The nonlinear behaviour begins once the particles start to unlink or split their bonds and crushed particles occupy the void spaces, as observed by Wang [92]. During the nonlinear behaviour, the brick material changes from cohesive to disjoint. In materials as clay, stone or concrete, the disjoined material cause a softening post-peak response with the expulsion of the outer parts. However, the 'Mo' '*wh*' and '*ha*' specimens showed a hardening nonlinear behaviour due to the confinement produced by the bearing surface treatment (grinded, capped with gypsum plaster or covered with gypsum powder) together with the reduced slenderness of the specimen (less than 0.4 h/w [59]). The developed confinement, after the expulsion of the outer parts of the specimen, prevents the inner material subject to triaxial compression from further expulsion. Finally, once the material has lost its cohesion within a state of confinement, the crushed particles start the rearrangement of their microstructure again, recompacting the material. This behaviour can be compared with that observed in confined sand tested in compression, as analysed by Nakata [93] who observed that the yielding characteristics depend on the grading curve. This behaviour can be associated with the increase in stiffness obtained in the final branch of the test, before reaching the load limit of the loading machine.

The considered representative points (1), (2), (3) and (4) can be related with meaningful effects with different stages in the behaviour of the specimens under compression. Points (1) and (2) are also identifiable in the specimens with a post-peak response before achieving the peak ultimate stress. Point (3) can be related with the descriptions of the second stage by Stroeven [87] and the third stage by Kotsovos [88,89], where cracks start to propagate and join in a stable manner. Point (4) shows a lateral expansion with widening cracks, as identified by Kotsovos [88,89]. Point (4) also indicates an inflexion point in the stress-displacement curve, denoting the beginning of a hardening response. Table 2 in Section 3.1 shows the equivalent compressive strength as derived from the reference values of the points 2, 3 and 4. In the following analysis reported in Section 4, the equivalent compressive strength estimated by point 4 of the grinded, capped with gypsum plaster and covered with gypsum powder specimens will be used.

4.2. Study of the influence of cross section's aspect ratio on the compressive strength

The experimental campaign on '*wh*' and '*ha*' specimens of both the mechanically extruded (Ex) and modern handmade units (Mo) allowed the comparison of the compressive strength in specimens with different cross-section aspect ratio and bearing surface treatment. The ratio between the shorter edge, the width (w), and the longer edge, the length (l), has been considered as the cross section's aspect ratio w/l. The cross section's aspect ratios w/l in the experimental campaign were 0.49 and 0.97 for 'Ex' '*wh*' and '*ha*', and 0.48 and 0.96 for 'Mo' '*wh*' and '*ha*'. The

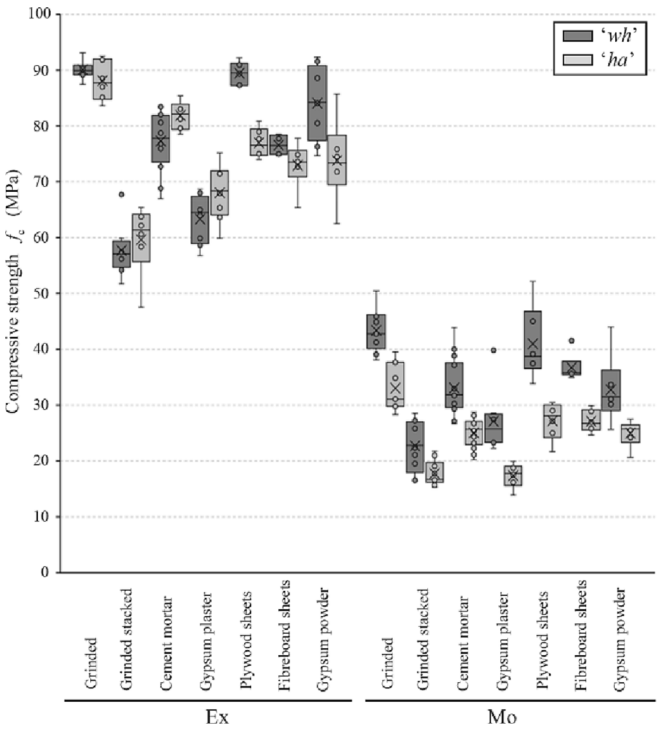

Fig. 7. Boxplot with '*wh*' and '*ha*' specimens' compressive strength values (f_c) for the 'Ex' and 'Mo' units with different bearing surface treatment. Inside the boxes, the medians are presented with a horizontal line and the averages are presented with an X.

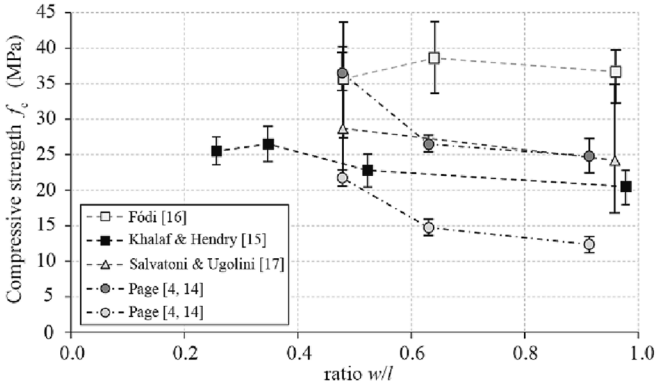

Fig. 8. Experimental compressive strength evaluated in specimens with different length/width ratio as found in five available experimental programs in the literature that tested solid units with different materials.

specimens tested with oiled PTFE leaves has not been considered in the analysis, since the experimental results in Section 3 show close values regardless of the specimen's shape.

Fig. 7 presents in a boxplot the distribution of the data based on the quartiles (being the second and third quartiles coloured inside the boxes), and shows the median (depicted as a horizontal line inside the box) and the average (depicted as a cross). As presented in Table 2 (Section 2) and in Fig. 7, the mean and median strength values for '*ha*' are higher than that for '*wh*' in the 'Ex' for stacked, capped with cement mortar and capped with gypsum plaster, while '*wh*' strength values are higher than that for '*ha*' in the 'Ex' for grinded, placed with birch plywood sheets, placed with fibreboard sheets and covered with gypsum powder. The 'Ex' specimens grinded and placed with fibreboard sheets, even if the '*wh*' mean and median are higher than '*ha*' ones, present the '*wh*' distribution within the upper distribution of '*ha*'. The mean and

median strength values for '*wh*' are higher than that for '*ha*' in the 'Mo' specimens.

The scientific literature discussed in Section 1 reports only a limited number of references dealing with the experimental testing of brick specimens in compression studying the cross section's aspect ratio influence. Fig. 8 shows experimental compressive strength values in specimens with different cross section's aspect ratio (*l/w*) obtained by Page [6,7], Khalaf and Hendry [5], Fódi [8] and Salvatoni and Ugolini [9]. The results from the references, including all the experimental values, are presented in a graph presented as a point (mean) with a line indicating the CV. Page [6,7] testing calcium silicate samples with plywood sheets obtained the highest strength for the lowest cross section's aspect ratio (*w/l*). Khalaf and Hendry [5], testing solid concrete bricks, also obtained the highest strength for the lowest *w/l*, and concluded that the length of the unit affects as the width. Khalaf and Hendry [5] proposed the experimental equation $\delta_{100} = (h/\sqrt{A})^{0.37}$ to obtain the shape factor referring to a cubic specimen of 100 mm edge, involving the specimen height (*h*) and the loading area (A). Fódi [8], after testing extruded solid fired clay bricks with grinded surfaces, obtained similar compressive strengths regardless of the *w/l* ratio, and concluded that the compressive strength depends on the width (smaller edge) and does not depend on the loaded area. Finally, Salvatoni and Ugolini [9], testing grinded modern handmade units, obtained, as Page [6,7] and Khalaf and Hendry [5], the highest compressive strength for the lowest *w/l* ratio. As explained in Section 4.1, in the specimens tested by Salvatoni and Ugolini [9] the compressive strength was calculated as the point of maximum secant slope due their hardening response. Thus, the literature review indicates that a cross section's aspect ratio (*w/l*) influence is normally observed in calcium silicate bricks, solid concrete bricks and handmade bricks. However, no apparent influence of the *w/l* ratio has been found in mechanically extruded bricks.

An in-depth analysis of the compressive strengths derived from the specimens with different cross section's aspect ratio (*w/l*) allows the detection of possible length influence in the mechanically extruded bricks (Ex) and modern handmade bricks (Mo). A correlation can be made between the compressive strength average of the specimens with the *w/l* aspect ratio close to 1.0 ('*ha*'), denoted by *fc_ha,* and the compressive strength average with the *w/l* aspect ratio close to 0.5 ('*wh*'), denoted by *fc_wh*. Table 3 shows the *fc_ha/fc_wh* correlations obtained from the experimental data derived from this research using different bearing surface treatments and from the scientific literature. For the specimens with hardening response, the compressive strength was estimated as proposed in Section 4.1. The mechanically extruded solid fired clay bricks ('Ex') show an experimental *fc_ha/fc_wh* ranging from 0.86 to 1.07, while Fódi [8] obtained 1.03. The concrete solid bricks tested by Khalaf and Hendry [5] showed *fc_ha/fc_wh* = 0.90. The modern handmade solid fired clay bricks ('Mo') show *fc_ha/fc_wh* ranging from 0.64 to 1.78, while Salvatoni and Ugolini [9] obtained 0.84. The calcium silicate bricks tested by Page [6,7] showed the lowest values of *fc_ha/fc_wh*, i.e. 0.57 and 0.68.

A significant influence of the cross section's aspect ratio (*w/l*) has been found in modern handmade bricks 'Mo', in which the highest compression strength is obtained in specimens with lower cross section's aspect ratio ('*wh*' specimen). This remarkable influence of the cross section's aspect ratio on the compressive strength of handmade bricks was also observed by Salvatoni and Ugolini [9], as well as by Khalaf and Hendry in moulded solid concrete units [5] and by Page in calcium silicate bricks [6,7]. Slight influence of the cross section's aspect ratio has been found in mechanically extruded solid clay bricks 'Ex', as also observed by Fódi in mechanically extruded bricks [8].

Table 3
fc_ha/fc_wh ratios of the experimental compressive strengths derived from specimens with aspect ratio close to 0.5 and 1.0, considering data from the current experimental program and from the literature. Values in brackets correspond to the Coefficients of Variation (CV).

fc_ha/fc_wh ratio		
	Ex	Mo
Grinded	0.98	0.76
Stacked	1.03	0.78
Cement mortar	1.06	0.76
Gypsum plaster	1.07	0.64
Plywood sheets	0.86	0.66
Fibreboard sheets	0.95	0.74
Gypsum powder	0.88	0.76
Average	0.97 [8.6%]	0.73 [7.6%]

References on scientific literature – ratio'$w/l \approx 1.0$' /' $w/l \approx 0.5$'

Fódi [8]	Khalaf & Hendry [5]	Page[6,7]	Page[6,7]	Salvatoni & Ugolini [9]
Mechanically extruded solid fired clay brick	Moulded solid concrete brick	Calcium silicate solid brick	Calcium silicate solid brick	Moulded handmade solid fired clay brick
1.03	0.90	0.68	0.68	0.84

4.3. Empirical correlation among compressive strengths derived from specimens with different bearing surface treatments

Based on the experimental campaign presented, this research has evaluated an empirical correlation between the compressive strengths derived from specimens with different bearing surface treatments ($f_{c,TR}$), making reference to the grinded surface treatment ($f_{c,GR}$) on '*wh*', '*ha*' and '*100*'. The grinded surface treatment is taken as reference since it produces the highest compressive strength value. Table 4 shows the following aspects: (1) the ratios between compressive strengths ($f_{c,TR}/f_{c,GR}$) seem to be higher for mechanically extruded bricks (Ex) than handmade bricks (Mo); (2) the ratios for specimens tested with two oiled PTFE have stepped values depending on the specimen's shape; (3) the ratios $f_{c,TR}/f_{c,GR}$ for each treatment seem to be influenced by the slenderness of the specimen, since each treatment seems to produce different amount of confinement; (4) specimens capped with gypsum plaster has the lowest $f_{c,TR}/f_{c,GR}$ ratio, except for '*C40*' specimens that exhibited lowest $f_{c,TR}/f_{c,GR}$ when covered with gypsum powder; (5) the ratios $f_{c,TR}/f_{c,GR}$ for the specimens capped with gypsum plaster or covered with gypsum powder are different for 'Ex' and 'Mo' units due to the different response depending on the brick type; (6) the specimens with plywood and fibreboard show higher $f_{c,TR}/f_{c,GR}$ ratios than '*C40*' specimens.

Table 4 presents, together with the results derived from the experimental program of the current research, the compressive strength ratios on fired clay bricks obtained from the experimental results of RILEM recommendations [78], Khalaf et al. [43], Templeton et al. [44], Morsy [42], already mentioned in the literature review of Section 1.

RILEM recommendations [78] specify that fired clay brick specimens grinded and capped with cement mortar bearing surface preparation exhibit different results, without quantifying such difference. Khalaf et al. [43] reported the compressive strength of whole hollow clay, frogged clay, and calcium silicate bricks, and concrete blocks with grinded surfaces, capped with mortar, with dental plaster, and placed with plywood sheets. The higher strength units (considered over 100 MPa) exhibited $f_{c,TR}/f_{c,GR} = 0.80$ for specimens grinded or capped with mortar, $f_{c,TR}/f_{c,GR}$ between 0.52 and 0.62 for specimens capped with dental plaster, and 0.66 for specimens with plywood sheets. For medium strength bricks, the $f_{c,TR}/f_{c,GR}$ ratios ranged between 0.94 and 1.07 for specimens capped with cement mortar, between 0.63 and 0.72 for specimens capped with dental plaster, and between 0.69 and 0.79 for specimens placed with plywood sheets. Templeton et al. [44] related the compressive strength of different types of modern clay bricks (mechanically extruded solid and perforated units, solid handmade and hydraulic pressed solid units) with grinded surface and capped with cement mortar. Templeton et al. [44] proposed the experimental

Table 4
Experimental ratios $f_{c,TR}/f_{c,GR}$ derived from the experimental program and from literature data. Values in brackets correspond to the Coefficients of Variation.

Origin		Mortar capped	Gypsum plaster	Plywood sheets	Fibreboard sheets	Gypsum powder	Oiled PTFE leaves
Experimental $f_{c,TR}/f_{c,GR}$							
Ex	'*wh*'	0.86	0.70	0.99	0.85	0.93	0.33
	'*ha*'	0.93	0.77	0.87	0.83	0.87	0.39
	'*100*'	0.79	0.73	1.00	0.95	1.00	0.49
	'*C40*'	0.74	0.58	1.28	1.33	0.48	0.71
Average 'Ex'		0.83 [10%]	0.70 [12%]	1.04 [17%]	0.99 [23%]	0.82 [28%]	–
Mo	'*wh*'	0.76	0.63	0.94	1.04	0.76	0.24
	'*ha*'	0.76	0.53	0.82	0.86	0.76	0.33
	'*100*'	0.81	0.40	0.95	0.90	0.64	0.37
	'*C40*'	1.02	0.92	1.26	1.54	0.41	0.69
Average 'Mo'		0.89 [12%]	0.64 [35%]	1.06 [17%]	1.09 [29%]	0.63 [25%]	–
References on literature reviewed $f_{c,TR}/f_{c,GR}$							
LUMA.1 [78]		different					
Khalaf et al. [43] [a]		0.80	0.52–0.62	0.66			
		0.94–1.07	0.63–0.72	0.69–0.79			
Templeton et al. [44]		0.78–0.80					
Morsy [42]				0.96–1.04	0.87–0.94 [b]		
Aubert et al. [49] [c]							0.98–1.07
RILEM TC148-SSC [39] [d]							0.37
							0.58–0.75
							0.57–1.17

[a] Hard strength brick first row, Soft strength brick second row.
[b] Hardboard.
[c] Specimen slenderness 1.00.
[d] Specimen slenderness 0.25 first row, 0.50 s row and 1.00 third row.

equation $f_{c,TR} = 0.707 \cdot f_{c,GR} + 8.534$ to relate the compressive strength between both treatments, obtaining $f_{c,TR}/f_{c,GR}$ ratios ranging between 0.78 and 0.80. Morsy [42] analysed ground and rough scaled clay units with seven types of bearing surface coating, i.e. steel, plywood, hardboard, 6 layers of polythene, rubber with fibres and pure rubber. The ratios between specimens tested with grinded surfaces and placed with plywood were 0.96 and 1.04, depending if the specimens tested with plywood had grinded or rough surfaces. The ratios with hardboard were between 0.87 and 0.94, depending on the direction of the fibres and if the specimen had grinded or rough surfaces.

Table 4 also considers available references dealing with bearing surface treatments in earth units (Aubert et al. [49]), and concrete specimens (RILEM TC 148-SSC [39]).

Aubert et al. [49], after placing 2 mm PTFE leaves on 50 × 50 × 50 mm^3 extruded earth bricks, observed experimental compressive strength similar to that of grinded specimens. The ratios range between 0.98 and 1.07. RILEM TC 148-SSC [39] for concrete indicates that the compressive strength in grinded specimens increases when the slenderness decrease below 2, except when oiled PTFE leaves are used. The thickness of the used oiled PTFE leaves in RILEM TC 148-SSC [39] are 50 mm, 100 mm, and 500 mm. The RILEM recommendations allow to found different $f_{c,TR}/f_{c,GR}$ ratios depending on the specimen slenderness, 0.37 for h/w of 0.25, 0.58 to 0.75 for h/w of 0.50, and 0.57 to 1.18 for h/w of 1.00.

The analysis of the $f_{c,TR}/f_{c,GR}$ ratios presented in Table 4 show important conclusions about the influence of the bearing surface treatment on the compressive strength of the investigated brick types. Overall, the results show a clear correlation between the compressive strength of each bearing surface treatment ($f_{c,TR}$) and of the grinded surface ($f_{c,GR}$) for both mechanically extruded (Ex) and modern handmade (Mo) brick samples. The experimental campaign exhibited similar ratios of those derived from data available in the scientific literature, yet enlarging the experimental database. The specimens capped with cement mortar have similar ratios of those investigated by Khalaf et al. [43] (0.80–1.07) and Templeton et al. [44] (0.78–0.80). The specimens capped with gypsum plaster have similar ratios of those investigated by Khalaf et al. [43] (0.52–0.72). The specimens with birch plywood and fibreboard sheets also have a similar ratio of those investigated by Morsy [42] (0.95–1.04 and 0.87–0.94), but differ from those studied by Khalaf et al. [43] for plywood sheets (0.69–0.79). The ratios close to 1.00 suggest that the lateral strains of the plywood and fibreboard were reduced as observed by Kleeman et al. [53]. It is noticed that the samples capped with gypsum plaster and covered with gypsum powder have different average $f_{c,TR}/f_{c,GR}$ depending on the brick type. There is no research available in the scientific literature comparing the compressive strength of grinded specimens with specimens covered with gypsum powder. The samples with oiled PTFE leaves have different ratios $f_{c,TR}/f_{c,GR}$ depending on the specimen's shape, since the influence of the specimen's slenderness seems to be attenuated as observed by RILEM TC 148-SSC [39]. RILEM TC 148-SSC [39] recommends the insertion of the oiled PTFE in concrete specimens to obtain similar strengths regardless of the specimen slenderness h/w. Although RILEM TC 148-SSC [39] remarks that the use of PTFE with a controlled application of oil can reduce the scattering, this research did not show any reduction in scattering with respect to the other proposed treatments (see Table 2).

Fig. 9 represents the results of the experimental program in a graphical manner, following the approach formulated by Morsy [52]. Different graphs refer different to types of unit ('Ex' or 'Mo') and specimens ('*wh*', '*ha*', '*100*', and '*C40*'). The relevant strength values for different surface treatments are reported on y-axis, while the x-axis can represent in a qualitative manner the amount of lateral restraint, as stated by Morsy. If we set the specimens with PTFE leaves as the reference ones, as PTFE leaves surface treatment showed similar compressive strengths regardless of the specimen shape, one can detect in a visual manner which treatments present a relative increase or decrease of the lateral restraint during compression testing. The specimens capped with cement mortar or gypsum plaster, or covered with gypsum powder, are more susceptible to variations of lateral restraint, as the restraint can either decrease for '*C40*' specimens or increase for the rest of specimens. The specimens with plywood or fibreboard sheets increase the lateral restraint regardless of the specimen type. The grinded specimens show the highest lateral restraint for '*wh*', '*ha*' and '*100*' specimens, except for '*C40*' specimens.

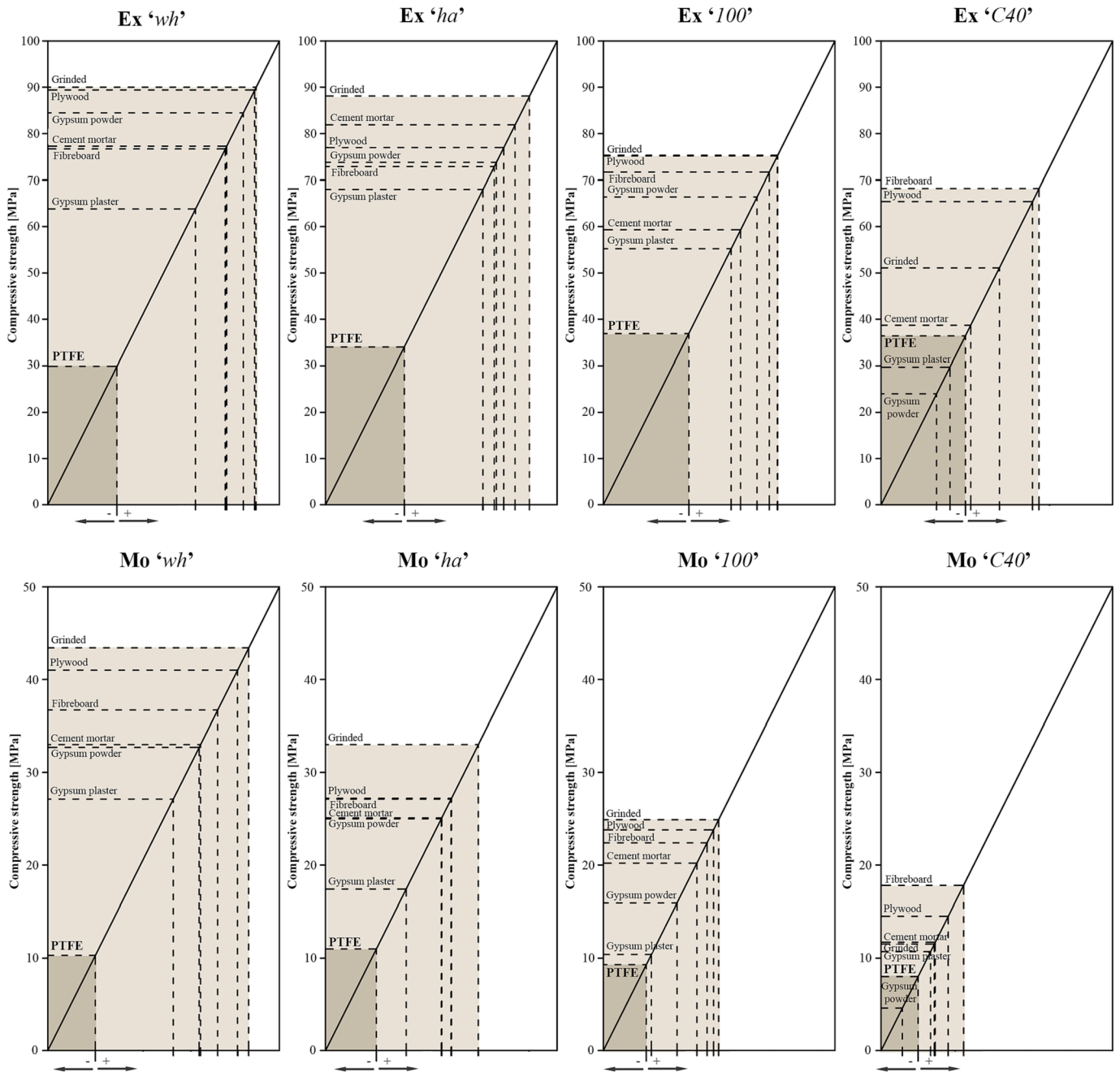

Fig. 9. Increase/decrease of the amount of lateral restraint according to different bearing surface treatments, making reference to specimens with oiled PTFE leaves.

4.4. Evaluation of the compressive strength according to different international standards

Fig. 10 shows the standard compressive strengths derived from the experimental campaign following the different international standard recommendations. The experimental average compressive strength obtained by testing all types of specimens with oiled PTFE leaves have been used as a reference, i.e. 34.3 MPa (10.4% CV) of 'Ex' and 9.5 MPa (20.2% CV) of 'Mo'. The European standard EN 772-1 + A1 [59] considers the use of the grinded specimens '*100*' and '2*ha*', and the specimen capped '*100*' with cement mortar. The experimental values have to be multiplied by a shape factor indicated in the Table A.1 of the standard, which is 0.7 for the '*100*' and 0.885 (interpolated value) for the '2*ha*'. Thus, the compressive strength according to the EN standard range between 41.5 MPa 52.7 MPa for 'Ex' and 14.1 to 17.4 MPa for 'Mo'. The American standard ASTM C67-21 [56] use the specimen '*ha*' capped with cement mortar or capped with gypsum plaster. The ASTM standard does not specify the use of any shape factor. The CAN/CSA A82:14 (R2018) [61] use the specimen '*wh*' and allow the specimen '*ha*' to test capped with gypsum plaster. The CAN/CSA does not specify the use of any shape factor either. The ASTM and CAN/CSA standard compressive strengths are the highest values, ranging between 63.8 and 81.9 MPa for 'Ex' and 17.4 to 27.1 MPa for 'MPa'. The Australian standard AS/NZS 4456.4 [60] use the specimen '*wh*' and allow the specimen '*ha*' to test placed with birch plywood sheets and fibreboard sheets. The experimental values require the use of an aspect ratio factor indicated in the standard, the interpolated 0.425 for 'Ex' and 0.375 for 'Mo' due to their different widths. The AS/NZS standard compressive strength are the lowest values, ranging between 31.0 and 38.0 MPa for 'Ex' and 10.2 to 15.4 MPa for 'Mo'. The AS/NZS values for '*ha*'

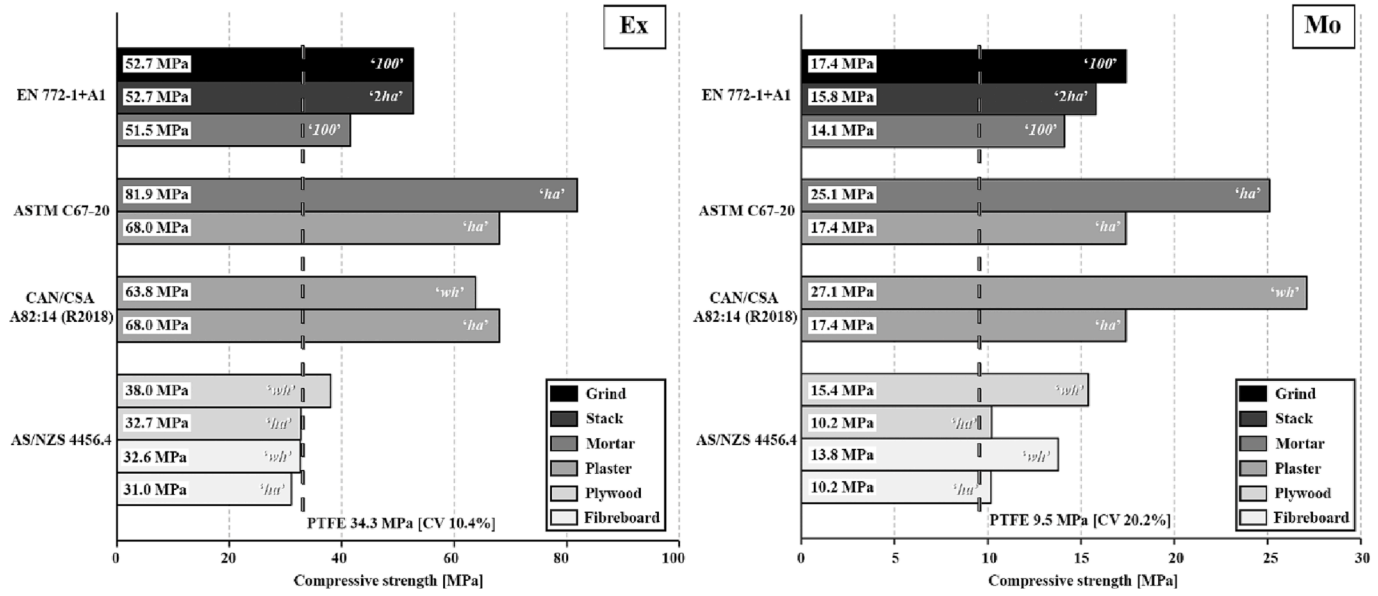

Fig. 10. Bar graph with the standard compressive strength of the references: European EN 772-1 + A1 [59], American ASTM C67-21 [56], Canadian CAN/CSA A82:14 (R2018) [61], and the Australian AS/NZS 4456.4 [60].

specimens tested with birch plywood or fibreboard sheets and 'Ex' '*wh*' tested with fibreboard have close standard compressive strength values than specimens tested with oiled PTFE leaves in both brick types.

5. Conclusions

This paper has presented novel experimental results about the compressive strength of fired clay brick solid samples with different shapes and surfaces treatments. A comprehensive experimental program considered a total amount of 458 specimens, derived from mechanically extruded (Ex) and modern handmade (Mo) bricks. The research has proposed first a novel method for the determination of the compressive strength in brick specimens with hardening response. Second, the paper has addressed the influence of the cross section's aspect ratio on the compressive strength. Third, the influence of bearing surface treatment has been analised indetail by investigating six different treatments, i.e. grinding, capping with cement mortar, capping with gypsum plaster, placement of plywood sheets, covering with gypsum powder, and covering with oiled PTFE leaves. Finally, the study has compared different methods of evaluating the compressive strength from the experimental measurements, according to different international standards for masonry testing. The following conclusions can be drawn from the analysis of the experimental results:

- The experimental tests on whole and half handmade brick specimens show a noticeable hardening response due to their low slenderness. allows simple method based on mathematical analysis of the stress-displacement experimental function is proposed to estimate the compressive strength.
- The experimental results and the scientific literature show that the cross section's aspect ratio is more influent in modern handmade solid fired clay bricks (Mo) than in mechanically extruded ones (Ex). The ratios between the strengths of the whole brick and the half brick ('*wh*'/'*ha*') ranged between 0.88 and 1.06 for 'Ex' specimens, and between 0.64 and 0.78 for 'Mo'.
- The compressive strength measured on the specimens with different bearing surface can be characterized by the ratio $f_{c,TR}/f_{c,GR}$ for slenderness under 0.4. The experimental ratio is 0.82 (CV of 8%) for specimens capped with cement mortar, and 0.93 (CV 7.5%) for specimens with birch plywood sheets, being similar to evidences available in the scientific literature. The experimental ratios $f_{c,TR}/f_{c,GR}$ of the specimens tested with gypsum material seem to be influenced both by the manufacturing process and the unit's strength unit. The ratio for 'Ex' specimens is 0.74 (CV of 4.7%) for capping with gypsum plaster, and 0.94 (CV of 6.7%) for covered with gypsum powder. The 'Mo' specimens present a ratio of 0.52 (CV 21.8%) for capping with gypsum plaster, and 0.72 (CV of 9.3%) for capping with gypsum powder.
- The capped specimens has exhibited varying amount of lateral restraint, depending of the scross section aspect ratio. Specimens tested with plywood and fiberboard sheets show high values regardless of the specimen shape. The amount of lateral restraint in specimens with grinded surfaces seems to be influenced mainly by the slenderness of the specimen.
- Capping with gypsum powder has shown compressive strength values similar to those of the grinded specimens, and those with plywood sheets for 'Ex' bricks, and similar to the specimens capped with cement mortar for 'Mo' bricks. The use of gypsum powder can hardly be considered as a low friction surface treatment, since the compression loading compacts the powder during the execution of the test, inducing a mechanical behaviour similar to that of capping.
- Testing the specimen placed with two oiled PTFE leaves has proved to be an advantageous technique for the evaluation of the unconfined compressive strength of solid fired clay units. This technique has shown similar compressive strength values regardless of the specimen shape.
- The standards for the evaluation of the compressive strength in bricks present a great variety of approaches. The American ASTM and the Canadian CAN/CSA provide the highest values of compressive strength, while the Australian AS/NZS provide the lowest values.

As this research has focused on solid fired clay bricks, future works could address the extension of the experimental database by including the application to different materials, such as mudbricks, fly ash clay bricks, concrete units, and calcium silicate bricks, as well as to other manufacturing processes, such as dry pressed into a mould or mechanically extruded in different directions. Another topic of future research may be studying the possible influence of other parameters on the compressive strength and the failure mechanisms, such as the material's porosity and the mineralogical composition.

CRediT authorship contribution statement

Albert Cabané: Conceptualization, Methodology, Validation, Formal analysis, Investigation, Resources, Data curation, Writing – original draft, Visualization. **Luca Pelà:** Conceptualization, Methodology, Validation, Investigation, Resources, Writing – review & editing, Supervision, Project administration, Funding acquisition. **Pere Roca:** Conceptualization, Methodology, Validation, Investigation, Resources, Writing – review & editing, Supervision, Project administration, Funding acquisition.

Declaration of Competing Interest

The authors declare that they have no known competing financial interests or personal relationships that could have appeared to influence the work reported in this paper.

Data availability

Data will be made available on request.

Acknowledgements

The authors gratefully acknowledge the financial support from the Ministry of Science, Innovation and Universities of the Spanish Government (MCIU), the State Agency of Research (AEI) as well as that of the ERDF (European Regional Development Fund) through the project SEVERUS (Multilevel evaluation of seismic vulnerability and risk mitigation of masonry buildings in resilient historical urban centres, ref. Num. RTI2018-099589-B-I00). Support from MCIU through a predoctoral grant awarded to the first author is also gratefully acknowledged.

References

[1] A.W. Hendry, Structural Masonry, Iowa State Univ. Bull. 59 (1998), https://doi.org/10.1007/978-1-349-14827-1.
[2] J. Segura, L. Pelà, P. Roca, Monotonic and cyclic testing of clay brick and lime mortar masonry in compression, Constr. Build. Mater. 193 (2018) 453–466, https://doi.org/10.1016/j.conbuildmat.2018.10.198.
[3] M. Van J.G.M., Strain-Softening of Concrete under Multiaxial Loading Conditions, Tech. Hogesch. Eindhoven. (1984). https://doi.org/10.6100/IR145193.
[4] A. Cabané, L. Pelà, P. Roca, Anisotropy and compressive strength evaluation of solid fired clay bricks by testing small specimens, Constr. Build. Mater. 344 (2022), 128195, https://doi.org/10.1016/j.conbuildmat.2022.128195.
[5] F.M. Khalaf, A.W. Hendry, Masonry unit shape factors from test results, in: Proc. Br. Mason. Soc., Stoke on Trent, 1994: pp. 136–139. https://www.masonry.org.uk/downloads/masonry-unit-shape-factors-from-test-results/.
[6] A.W. Page, A study of the influence of brick size on the compressive strength of calcium silicate masonry, University of Newcastle Faculty of Engineering, 1984.
[7] A.W. Page, R. Marshall, The influence of brick and brickwork prism aspect ratio on the evaluation of compressive strength, in: Proc. 7th Int, Brick Block Mason. Conf, Melbourne, Australia, 1985, pp. 653–664.
[8] A. Fódi, Effects influencing the compressive strength of a solid, fired clay brick, Period. Polytech. Civ. Eng. 55 (2011) 117, https://doi.org/10.3311/pp.ci.2011-2.04.
[9] P. Salvatoni, M. Ugolini, Comportamento di elementi in muratura fino a collasso: prove sperimentali e modellazione numerica, Politecnico di Milano (2016). https://www.politesi.polimi.it/bitstream/10589/133545/3/2017_04_Ugolini_Salvatoni.pdf.
[10] W.M. Murray, Discussion, in: ASTM Proc., American Society for Testing and Materials (ASTM), 1942: pp. 1047–1048.
[11] H.K. Hilsdorf, Die Bestimmung der zweiachsigen Festigkeit des Betons, Schriftenr. Des DAfStb. 173 (1965) 68.
[12] H. Kupfer, H.K. Hilsdorf, H. Rusch, Behavior of concrete under biaxial stresses, ACI J. Proc. 66 (1969) 656–666. https://doi.org/10.14359/7388.
[13] K. Thomas, D.C. O'Leary, Tensile Strength Tests on Two Types of Brick, in: 2nd Int. Brick Block Mason. Conf., Stoke-on-Trent, England, 1970: pp. 69–74. http://www.hms.civil.uminho.pt/ibmac/1970/69.pdf.
[14] L. Binda, G. Mirabella Roberti, C. Tiraboschi, S. Abbaneo, Measuring masonry material properties, in: Proc. U.S.-Italy Work. Guidel. Seism. Eval. Rehabil. Unreinforced Mason, Build., National Center for Earthquake Engineering Research, Pavia, Italy, 1994, pp. 326–347.
[15] L. Binda, C. Tiraboschi, S. Abbaneo, Experimental research to characterise masonry materials, Mason. Int. 10 (1997) 92–101.
[16] A.W. Page, P.W. Kleeman, The influence of capping material and platen restraint on the failure of hollow masonry units and prisms, in: Proc. Ninth Int. Brick/Block Mason. Conf., Berlin, 1991: pp. 662–670.
[17] A. Hussein, H. Marzouk, Finite element evaluation of the boundary conditions for biaxial testing of high strength concrete, Mater. Stuctures. 33 (2000) 299–308, https://doi.org/10.1007/BF02479700.
[18] G. Schickert, On the influence of different load application techniques on the lateral strain and fracture of concrete specimens, Cem. Concr. Res. 3 (1973) 487–494, https://doi.org/10.1016/0008-8846(73)90087-2.
[19] G. Schickert, H. Winkler, Versuchsergebnisse Zur Festigkeit Und Verformung Von Beton Bei Mehraxialer Druckbeanspruchung, Dtsch Ausschuss Stahlbet. (1977). https://opus4.kobv.de/opus4-bam/frontdoor/index/index/year/2015/docId/404.
[20] G. Schickert, Schwellenwerte beim Betondruckversuch, Dtsch. Ausschuss Fuer Stahlbet. (1980). https://opus4.kobv.de/opus4-bam/frontdoor/index/index/year/2015/docId/380.
[21] H.F. Gonnerman, Effect of end condition of cylinder on compressive strength of concrete, ASTM Proc. 24. Part I (1924) 1036–1065. https://catalog.hathitrust.org/Record/102103985.
[22] W.F. Purrington, J. McCornick, A Simple Device to obviate Capping of Concrete Specimens, in: ASTM Proc., American Society for Testing and Materials (ASTM), 1926: pp. 488–492.
[23] D.D. McGuire, Testing Concrete Cylinders Using Confined Sand Cushion, in: ASTM Proc., American Society for Testing and Materials (ASTM), 1930: pp. 515–517.
[24] P.J. Freeman, Capping Device for Concrete Cylinders, in: Eng. News-Record, 1928: p. 111.
[25] P.J. Freeman, Method of Capping Concrete Cylinders Using Sulfur Compound, in: ASTM Proc., American Society for Testing and Materials (ASTM), 1930: pp. 518–520.
[26] G.E. Troxell, The Effect of Capping Methods and End Conditions Before Capping Upon Compressive Strength of Concrete Test Cylinders, in: ASTM Proc., American Society for Testing and Materials (ASTM), 1941: pp. 1039–1052.
[27] E.N. Vidal, R.F. Blanks, Absorbtive Form Lining, in: Int. Concr. Abstr. Portal - J. Proc., 1942: pp. 253–268. https://www.concrete.org/publications/internationalconcreteabstractsportal/m/details/id/8600.
[28] F.M. Masters, A.C. Loewer, The Effects of Capping Materials on the Apparent Strength of Concrete Specimens, in: AS, American Society for Testing and Materials (ASTM), 1952: pp. 30–36.
[29] G. Werner, The Effect of Capping Material on the Compressive Strength of Concrete Cylinders, in: ASTM Proc., American Society for Testing and Materials (ASTM), 1958: pp. 1166–1186.
[30] K.L. Saucier, Effect of Method of Preparation of Ends of Concrete Cylinders for Testing, U S Army Eng Waterw Exp Stn, Misc Pap C-72-12. (1972).
[31] C. Ozyildirim, Neoprene pads for capping concrete cylinders, Cem. Concr. Aggregates 7 (1985) 25, https://doi.org/10.1520/CCA10040J.
[32] P.M. Carrasquillo, R.L. Carrasquillo, Effect of using unbonded capping systems on the compressive strength of concrete cylinders, Mater. J. 85 (1987) 141–147. https://www.concrete.org/publications/internationalconcreteabstractsportal/m/details/id/1799.
[33] D. Richardson, Effects of testing variables' effects on the comparison of neoprene pad and sulfur mortar-capped concrete test cylinders, ACI Mater. J. 87 (1990) 489–495. https://www.concrete.org/publications/internationalconcreteabstractsportal.aspx?m=details&i=1890.
[34] B. Chojnacki, P. Read, Compressive Strength Test Procedures for Testing High Strength Concrete: Final Report, (1991).
[35] M.F. Pistilli, T. Willems, Evaluation of cylinder size and capping method in compression strength testing of concrete, Cem. Concr. Aggregates. 15 (1993), https://doi.org/10.1520/CCA10588J.
[36] M. Lessard, O. Challal, P.-C. Aticin, Testing high-strength concrete compressive strength, Mater. J. 90 (1993) 303–307. https://www.concrete.org/publications/internationalconcreteabstractsportal/m/details/id/3876.
[37] C.W. French, A. Mokhtarzadeh, High strength concrete: effects of materials, curing and test procedures on short-term compressive strength, PCI J. 38 (1993) 76–87. https://doi.org/10.15554/pcij.05011993.76.87.
[38] N.J. Carino, G. William F., Effects of Testing Variables on the Measured Compressive Strength of High-Strength (90 MPa) Concrete, National Bureau of Standards, Gaithersburg, Maryland, 1994. https://nvlpubs.nist.gov/nistpubs/Legacy/IR/nistir5405.pdf.
[39] J.G.M. van Mier, S.P. Shah, M. Arnaud, J.P. Balayssac, A. Bascoul, S. Choi, D. Dasenbrock, G. Ferrara, C. French, M.E. Gobbi, B.L. Karihaloo, G. König, M. D. Kotsovos, J. Labuz, D. Lange-Kornbak, G. Markeset, M.N. Pavlovic, G. Simsch, K.-C. Thienel, A. Turatsinze, M. Ulmer, H.J.G.M. van Geel, M.R.A. van Vliet, D. Zissopoulos, Strain-softening of concrete in uniaxial compression, Mater. Struct. 30 (1997) 195–209, https://doi.org/10.1007/BF02486177.
[40] N.W. Kelch, F.E. Emme, Effect of type, thickness, and age of capping compounds on the apparent compressive strength of brick, ASTM Bull. 230 (1958) 38–41.
[41] C.M. Dodd, T.D. McGee, A comparison of various methods of capping brick, structural tile, and concrete block for compressive strength tests, Iowa State Univ. Bull. 59 (1960) 1–11. https://iucat.iu.edu/catalog/6584165.
[42] E.H. Morsy, Mortar properties influencing brickwork strength - Chapter 6: The influence of end and joint conditions of different rigidities on the failure characteristics of bricks and brick masonry, University of Edimburg, 1968.
[43] F.M. Khalaf, A.W. Hendry, Effect of bed-face preparation in compressive testing of masonry units, in: Proc. 2nd Int, Mason. Conf, London, 1989, pp. 129–130.
[44] W. Templeton, G.J. Edgell, The compressive strength of clay bricks ground or mortar capped, Mason. Int. 4 (1990) 66–67. https://www.masonry.org.uk/downloads/the-compressive-strength-of-clay-bricks-ground-or-mortar-capped/.

[45] International Standard, ISO 9652 Masonry - Part 4: Test methods (Withdrawn), (2000).
[46] R.G. Drysdale, A.A. Hamid, L.R. Baker, Masonry Materials, in: Prentice-Hall Inc. (Ed.), Mason. Struct. Behav. Des., Englewood Cliffs, New Jersey, 1994: pp. 112–181.
[47] L. Crouch, M. Knight, R. Henderson, W. Sneed, Unbonded Capping for Concrete Masonry Units, Mason, Mater. Testing, Appl. (1999) 62–74, https://doi.org/10.1520/STP14201S.
[48] P.B. Lourenço, F.M. Fernandes, F. Castro, Handmade clay bricks: chemical, physical and mechanical properties, Int. J. Archit. Herit. 4 (2010) 38–58, https://doi.org/10.1080/15583050902871092.
[49] J.E. Aubert, P. Maillard, J.C. Morel, M. Al Rafii, Towards a simple compressive strength test for earth bricks? Mater. Struct. 49 (2016) 1641–1654, https://doi.org/10.1617/s11527-015-0601-y.
[50] I.M. Daniel, A.J. Durelli, Photothermoelastic analysis of bonded propellant grains, Exp. Mech. 1 (1961) 97–104, https://doi.org/10.1007/BF02324072.
[51] A.M. Neville, Properties of concrete, Pearson Education Limited, 2011.
[52] G.C. Braga, L.C. Mendes, Analysis of neoprene bearings on requests and strains, Int. J. Appl. Eng. Res. 15 (2020) 40–47. https://www.ripublication.com/ijaer20/ijaerv15n1_06.pdf.
[53] P.W. Kleeman, A.W. Page, The in-situ properties of packing materials used in compression tests, Mason. Int. 4 (1990) 68–74.
[54] J. Nichols, Y. Totoev, Experimental determination of the dynamic Modulus of Elasticity of masonry units, 15th Aust Conf. Mech. Struct. Mater. (2013) 1–7.
[55] N. Makoond, L. Pelà, C. Molins, Dynamic elastic properties of brick masonry constituents, Constr. Build. Mater. 199 (2019) 756–770, https://doi.org/10.1016/j.conbuildmat.2018.12.071.
[56] American Society for Testing and Materials (ASTM), C67/C67M-21 Standard Test Methods for Sampling and Testing Brick and Structural Clay Tile, (2021). https://doi.org/10.1520/C0067_C0067M-21.
[57] American Society for Testing and Materials (ASTM), C140/C140M-22b Standard test methods for Sampling and Testing Concrete Masonry Units and Related Units, (2022). https://doi.org/10.1520/C0140-13.
[58] American Society for Testing and Materials (ASTM), C1552-16 Standard Practice for Capping Concrete Masonry Units, Related Units and Masonry Prisms for Compression Testing, (2016). https://doi.org/10.1520/C1552-16.
[59] European Committee for Standardization (CEN), EN 772-1:2011+A1:2016 Methods of test for Masonry Units - Part 1: Determination of Compressive Strength, (2016).
[60] Australian Standards, AS/NZS 4456.4 Masonry units and segmental pavers and flags - Methods of test Determining compressive strength of masonry units, (2003).
[61] Standards Council of Canada, CAN/CSA A82:14 (R2018) Fired masonry brick made from clay or shale, (2018). https://www.csagroup.org/store/product/CAN%25100CSA-A82-14/.
[62] Standards Council of Canada, CAN/CSA A165 SERIES-14 (R2019) Standards on concrete masonry units, (2019). https://www.csagroup.org/store/product/2702048/.
[63] American Society for Testing and Materials (ASTM), C39/C39M-21 Standard Test Method for Compressive Strength of Cylindrical Concrete Specimens, (2021). http://www.astm.org/cgi-bin/resolver.cgi?C39C39M.
[64] American Society for Testing and Materials (ASTM), C617-10 Standard Practice for Capping Cylindrical Concrete Specimens, (2010). https://doi.org/10.1520/C0617-10.
[65] American Society for Testing and Materials (ASTM), C1231/C1231M-14: Standard Practice for Use of Unbonded Caps in Determination of Compressive Strength of Hardened Concrete Cylinders, (2014). https://doi.org/10.1520/C1231_C1231M-14.
[66] European Committee for Standardization (CEN), EN 12390-3:2020 Testing hardened concrete. Part 3: Compressive strength of test specimens, (2020).
[67] Deutsche Norm, DIN 18555-9:2019-04 Testing of mortar containing mineral binders - Part 9: Determining the compressive strength of hardened mortar, (2019).
[68] L. Pelà, P. Roca, A. Aprile, Combined in-situ and laboratory minor destructive testing of historical mortars, Int. J. Archit. Herit. 12 (2018) 334–349, https://doi.org/10.1080/15583058.2017.1323247.
[69] J. Ghadami, M. Nematzadeh, Effect of bond shear stress on compressive behaviour of steel tube-confined concrete with active and passive confinement, Eur. J. Environ. Civ. Eng. 22 (2018) 783–810, https://doi.org/10.1080/19648189.2016.1219878.
[70] European Committee for Standardization (CEN), EN 772-16:2011 Methods of test for masonry units - Part 16: Determination of dimensions, (2011).
[71] European Committee for Standardization (CEN), EN 772-13:2001 Methods of test for masonry units. Part 13: Determination of net and gross dry density of masonry units (except for natural stone), (2001).
[72] European Committee for Standardization (CEN), EN 772-3:1999 Methods of test for masonry units. Part 3: Determination of net volume and percentage of voids of clay masonry units by hydrostatic weighing, (1999).
[73] European Committee for Standardization (CEN), EN 772-4 Methods of test for masonry units. Part 4: Determination of real and bulk density and of total and open porosity for natural stone masonry units, (1999).
[74] European Committee for Standardization (CEN), EN 772-21:2011 Methods of test for masonry units. Part 21: Determination of water absorption of clay and calcium silicate masonry units by cold water absortion, (2011).
[75] European Committee for Standardization (CEN), EN 772-11 Methods of test for masonry units. Part 11: Determination of water absorption of aggregate concrete, autoclaved aerated concrete, manufactured stone and natural stone masonry units due to capillary action and the initial rate of water absorption, (2011).
[76] N. Makoond, A. Cabané, L. Pelà, C. Molins, Relationship between the static and dynamic elastic modulus of brick masonry constituents, Constr. Build. Mater. 259 (2020), 120386, https://doi.org/10.1016/j.conbuildmat.2020.120386.
[77] Bureau of Indian Standards, IS 3495 Methods of Tests of Burnt Clay building brick - Part 1: Determination of compressive strength, (2002).
[78] R. Bartusch, F. Händle, Laminations in Extrusion, in: F. Händle (Ed.), Extrus. Ceram. Eng. Mater. Process., Springer, Berlin, Heidelberg, 2009: pp. 187–210. https://doi.org/10.1007/978-3-540-27102-4_10.
[79] A. Delibes, G. Gonzalez, Estudio de la influencia que los distintos tipos de refrentado ejercen en el ensayo a compresión de probetas de hormigón, Inf. La Construcción. 29 (1976) 67–73. https://informesdelaconstruccion.revistas.csic.es/index.php/informesdelaconstruccion/article/view/2745/3055.
[80] R. Hooton, C. Lobo, G. Mullings, R. Gaynor, Effect of capping materials and procedures on the measured compressive strength of high-strength concrete, Cem. Concr. Aggregates 16 (1994) 173, https://doi.org/10.1520/CCA10296J.
[81] D.N. Richardson, Effects of testing variables on the comparison of neoprene pad and sulfur mortar-capped concrete test cylinders, ACI Mater. J. 87 (1990) 489–495. https://doi.org/10.14359/1890.
[82] ACICommittee 234, ACI 234R-96 Guide for the Use of Silica Fume in Concrete, (2000).
[83] European Committee for Standardization (CEN), EN 1015-11:2020 Methods of test for mortar for masonry - Part 11: Determination of flexural and compressive strength of hardened mortar, (2020).
[84] R. Bartusch, F. Händle, Laminations in Extrusion, in: F. Händle (Ed.), Extrus. Ceram. Eng. Mater. Process., Springer, Berlin, Heidelberg, 2009: pp. 187–210. https://doi.org/10.1007/978-3-540-27102-4_10.
[85] A. Viani, R. Ševčík, M.-S. Appavou, A. Radulescu, Evolution of fine microstructure during firing of extruded clays: A small angle neutron scattering study, Appl. Clay Sci. 166 (2018) 1–8, https://doi.org/10.1016/j.clay.2018.09.002.
[86] K.J. Krakowiak, P.B. Lourenço, F.J. Ulm, Multitechnique investigation of extruded clay brick microstructure, J. Am. Ceram. Soc. 94 (2011) 3012–3022, https://doi.org/10.1111/j.1551-2916.2011.04484.x.
[87] P. Stroeven, Geometric probability approach to the examination of microcracking in plain concrete, J. Mater. Sci. 14 (1979) 1141–1151, https://doi.org/10.1007/BF00561298.
[88] M.D. Kotsovos, Fracture processes of concrete under generalised stress states Fracture processes of concrete under generalised stress states, Matériaux Constr. 12 (1979) 431, https://doi.org/10.1007/BF02476287.
[89] M.D. Kotsovos, Failure criteria for concrete under generalised stress states, Imperial College of Science and Technology of London, 1974.
[90] F.M. Fernandes, P.B. Lourenço, F. Castro, Ancient clay bricks: manufacture and properties, in: Mater. Technol. Pract. Hist. Herit, Struct., Springer, Netherlands, Dordrecht, 2010, pp. 29–48, https://doi.org/10.1007/978-90-481-2684-2_3.
[91] F.M.C.P. Fernandes, Evaluation of two novel NDT techniques: Microdrilling of clay bricks and Ground Penetrating Radar in masonry, Universidade do Minho (2006). https://doi.org/10.29327/549675.
[92] G. Wang, X. Zhang, X. Liu, Y. Xu, J. Lu, Microscopic evolution of pore characteristics and particle orientation of granite residual soil in one-dimensional compression, Geofluids 2022 (2022) 1–13, https://doi.org/10.1155/2022/8380656.
[93] Y. Nakata, M. Hyodo, A.F.L. Hyde, Y. Kato, H. Murata, Microscopic particle crushing of sand subjected to high pressure one-dimensional compression, Soils Found. 41 (2001) 69–82, https://doi.org/10.3208/sandf.41.69.